Received: 6 October 2023 | Revised: 29 February 2024 | Accepted: 27 March 2024

DOI: 10.1111/gbi.12597

ORIGINAL ARTICLE

gebiology WILEY

Deep-water first occurrences of Ediacara biota prior to the Shuram carbon isotope excursion in the Wernecke Mountains, Yukon, Canada

Thomas H. Boag[1,2,3] | James F. Busch[4] | Jared T. Gooley[5] | Justin V. Strauss[4] | Erik A. Sperling[1]

[1]Department of Earth and Planetary Science, Stanford University, Stanford, California, USA

[2]Department of Earth and Planetary Sciences, Yale University, New Haven, Connecticut, USA

[3]Department of Geosciences, Princeton University, Princeton, New Jersey, USA

[4]Department of Earth Sciences, Dartmouth College, Hanover, New Hampshire, USA

[5]Alaska Science Center, U.S. Geological Survey, Anchorage, Alaska, USA

Correspondence
Thomas H. Boag and Erik A. Sperling, Department of Earth and Planetary Science, Stanford University, Stanford, CA 94305, USA.
Email: tom.boag@gmail.com and esper@stanford.edu

Funding information
Natural Sciences and Engineering Research Council of Canada; National Science Foundation, Grant/Award Number: EAR-1654131 and EAR-2021176; National Geographic Society, Grant/Award Number: CP-102R-17; Stanford Project on Deepwater Depositional Systems; Geological Society of America; American Philosophical Society

Abstract

Ediacara-type macrofossils appear as early as ~575 Ma in deep-water facies of the Drook Formation of the Avalon Peninsula, Newfoundland, and the Nadaleen Formation of Yukon and Northwest Territories, Canada. Our ability to assess whether a deep-water origination of the Ediacara biota is a genuine reflection of evolutionary succession, an artifact of an incomplete stratigraphic record, or a bathymetrically controlled biotope is limited by a lack of geochronological constraints and detailed shelf-to-slope transects of Ediacaran continental margins. The Ediacaran Rackla Group of the Wernecke Mountains, NW Canada, represents an ideal shelf-to-slope depositional system to understand the spatiotemporal and environmental context of Ediacara-type organisms' stratigraphic occurrence. New sedimentological and paleontological data presented herein from the Wernecke Mountains establish a stratigraphic framework relating shelfal strata in the Goz/Corn Creek area to lower slope deposits in the Nadaleen River area. We report new discoveries of numerous *Aspidella* hold-fast discs, indicative of frondose Ediacara organisms, from deep-water slope deposits of the Nadaleen Formation stratigraphically below the Shuram carbon isotope excursion (CIE) in the Nadaleen River area. Such fossils are notably absent in coeval shallow-water strata in the Goz/Corn Creek region despite appropriate facies for potential preservation. The presence of pre-Shuram CIE Ediacara-type fossils occurring only in deep-water facies within a basin that has equivalent well-preserved shallow-water facies provides the first stratigraphic paleobiological support for a deep-water origination of the Ediacara biota. In contrast, new occurrences of Ediacara-type fossils (including juvenile fronds, *Beltanelliformis*, *Aspidella*, annulated tubes, and multiple ichnotaxa) are found above the Shuram CIE in both deep- and shallow-water deposits of the Blueflower Formation. Given existing age constraints on the Shuram CIE, it appears that Ediacaran organisms may have originated in the deeper ocean and lived there for up to ~15 million years before migrating into shelfal environments in the terminal Ediacaran. This indicates unique ecophysiological constraints likely shaped the initial habitat preference and later environmental expansion of the Ediacara biota.

https://doi.org/10.1111/gbi.12597

1 | INTRODUCTION

The Ediacara biota represents the earliest uncontroversial large and complex multicellular eukaryotes in the fossil record. Their first occurrences are known exclusively from deep water (slope and basinal) deposits from the Avalon Peninsula in Newfoundland, Canada (Narbonne & Gehling, 2003), Charnwood Forest in England (Wilby et al., 2011), and the Mackenzie and Wernecke Mountains of NW Canada (e.g., Moynihan et al., 2019; Narbonne et al., 2014; Sperling et al., 2016). These fossil occurrences are colloquially referred to as the “Avalon assemblage” and contain diverse sessile frond-like organisms with fractal morphologies divided into several groups, including rangeomorphs and arboreomorphs (Liu et al., 2015; Xiao & Laflamme, 2009), as well as other fossils tentatively interpreted to be cnidarians (Liu et al., 2014) and sponges (Sperling et al., 2011). The Avalon assemblage achieves maximal diversity and disparity in deep-water successions which have been dated to ~574–560 Ma (Canfield et al., 2020; Matthews et al., 2020; Noble et al., 2015; Pu et al., 2016). These Avalon-type organisms also appear in shallow-water shelf environments later in the Ediacaran, albeit in lower diversity (Grazhdankin, 2014). Temporally longer-ranging fronds co-occur alongside highly diverse Ediacaran groups in ca. 560–550 Ma shallow-water strata of Australia and Russia (known as the “White Sea assemblage”), including the earliest bilaterian trace fossils and taxa variously described as animals such as *Dickinsonia*, *Kimberella*, and *Ikaria* (Evans et al., 2020; Fedonkin, 2003; Gehling & Droser, 2013; Sperling & Vinther, 2010). Few frondose Ediacaran taxa extend into depauperate terminal ca. 549–539 Ma Ediacaran ecosystems, which also include increasingly complex metazoan trace and tubular fossils. This interval is colloquially known as the “Nama assemblage” (Darroch et al., 2018, 2021). These frondose species ultimately went extinct alongside the rest of the Ediacara biota at the ca. 538 Ma Ediacaran-Cambrian boundary (Darroch et al., 2015; Smith et al., 2016; Muscente et al., 2018; Bowyer et al., 2022; Nelson et al., 2022, 2023; though this boundary may be as young as 533 Ma (Nelson et al., 2023)).

A major unanswered question in Ediacaran paleobiology is whether the first Avalon assemblage organisms truly originated in deep-water, and if so, what environmental conditions may have influenced this evolutionary cradle. Although exact water depths are difficult to quantify, the first Avalon fossil occurrences in the Drook Formation of Newfoundland occur in a turbidite-dominated basin-floor to lower-middle fan settings, likely representing >1 km water depth (Gardiner, 1984; Wood et al., 2003), while the first appearances in NW Canada occur in slope settings estimated to have been deposited >750 m deep and more likely at ~1000–1500 m depths (Dalrymple & Narbonne, 1996). From an environmental standpoint, there is little to offer for animals in such settings compared to shallow water (discussed by Boag et al. (2018))—the deep ocean is cold, dark, and unchanging, and has inherently lower food supply and oxygen than shallow-water settings. Sinking organic matter is rapidly remineralized in the upper ocean (Marsay et al., 2015), and there is consequently limited chemical energy (e.g., organic carbon) delivered to the deep-sea benthos. Today, the modern deep ocean contains depressed species-level diversity, primarily because of the limited food supply (Smith et al., 2008; Woolley et al., 2016). Because this organic carbon remineralization occurs through aerobic respiration, oxygen partial pressures in the deep ocean are never higher than in shallow seas in direct gas exchange with the atmosphere. There is also little or no sunlight, which prohibits benthic algae as a food source for grazers. Further, an evolutionary appearance in the deep sea would contrast with patterns observed in Phanerozoic animal evolution, wherein major ecological innovations usually appeared in nearshore environments and then expanded to deeper-water depths (Jablonski et al., 1983). Thus, if the Avalon assemblage did first appear in the deeper ocean (Narbonne et al., 2014), this represents an evolutionary and environmental conundrum.

Fortunately, geochronological data have helped clarify the timing of Ediacaran fossil origination and the relationship to major environmental changes, including regional glaciation(s) and the Shuram carbon isotope excursion (CIE). Radiometric ages from Newfoundland constrain glacial deposits of the Gaskiers Formation to between 580.90 ± 0.40 and 579.24 ± 0.17 Ma, representing a duration of <340 thousand years (Pu et al., 2016; although the glaciation may have extended beyond this, Fitzgerald et al., 2024). The Shuram CIE, which is present in Ediacaran strata globally across six paleocontinents, represents the most negative CIE in Earth's history. Despite documentation of the Shuram CIE in widespread localities, there remain key uncertainties regarding its causal driver (Bergmann, Osburn, et al., 2022; Busch et al., 2022; Fike et al., 2006; Li et al., 2017) and the possible association with major changes in marine redox conditions (Gong et al., 2023; Ostrander, 2023; Zhang et al., 2019). Recently, new geochronological studies have provided a revised temporal framework for the Shuram excursion (Canfield et al., 2020; Matthews et al., 2020; Rooney et al., 2020). Re-Os dates from the Wernecke and Ogilvie Mountains (both NW Canada) and Oman constrain the age of the Shuram CIE to ca. 574–567 Ma (Rooney et al., 2020), suggesting that the Shuram excursion occurs entirely within the Avalon assemblage and predates the White Sea assemblage altogether. Zircon U–Pb dates from fossiliferous Ediacaran strata of the Conception Group in Newfoundland independently agree with these Re-Os ages (Matthews et al., 2020). The Conception Group ages bound a carbonate carbon isotope profile with similar amplitude and pattern to the Shuram CIE (Canfield et al., 2020), although these isotopic data were measured from trace carbonate in siliciclastic-dominated rocks and may have an authigenic origin. Combined, these radiometric constraints present a new opportunity to examine evolutionary trends in the Ediacaran fossil record.

Unfortunately, many of the Ediacaran's earliest fossiliferous locales occur in basins where only one major paleoenvironment is preserved. This is especially true in early Avalon assemblages, such as those in Newfoundland, Canada, and England (and to some extent in the Mackenzie Mountains; see below), which were deposited in deep-water settings and where no regional up-dip shallow-water deposits of equivalent age are exposed to search for comparable fossils (Boag et al., 2016; Ichaso et al., 2007; Narbonne et al., 2014). This fundamental issue has limited our understanding of many major questions in Ediacaran paleobiology, such as when the Ediacara biota appear in the fossil record, the details of the Avalon-White Sea transition, whether the Ediacara biota evolved in the shallow or deep ocean, and when and why early animals seemingly later radiated up onto continental shelves. Answering such questions requires analysis of fossil appearances using stratigraphic and paleobiologic methods that have been employed for Phanerozoic intervals (Holland, 1995; Patzkowsky & Holland, 2012). In this study, we present new data from an extensive shelf-to-basin stratigraphic framework spanning the Ediacaran Period in the Wernecke Mountains, Yukon, Canada (Figure 1). These data allow us to utilize this stratigraphic paleobiological approach to determine whether Ediacaran organisms did indeed originate in the deeper ocean during the Avalon interval before radiating up onto continental shelves and whether environmental drivers may have played a role in this pattern.

1.1 | Geological and paleontological background

Stratigraphic sections examined in this study occur in the Wernecke Mountains, located in central Yukon, ~400 km NNE of Whitehorse (Figure 1). Ediacaran strata of the Rackla Group in the Wernecke Mountains are part of a wider succession of Neoproterozoic to Cambrian strata exposed in the North American Cordillera known as the Windermere Supergroup (Moynihan et al., 2019, and references therein) (Figure 2). These rocks were deposited in multiple subbasins along the Laurentian margin due to protracted rifting of the supercontinent Rodinia in the Tonian and Cryogenian periods, with final rifting occurring during the late Ediacaran–middle Cambrian (Bond et al., 1985; Moynihan et al., 2019; Strauss et al., 2015).

Previous investigations of the Wernecke Mountains have led to the identification of an Ediacaran mixed siliciclastic and carbonate succession that records the transition from inner shelf or platform to slope facies along a present-day north-to-south transect, specifically from the Goz/Corn Creek area (proximal or shallow water) to the Nadaleen River region (distal or deep water) (Busch et al., 2022, 2023; Macdonald et al., 2013; Moynihan et al., 2019; Pyle et al., 2004) (Figure 1). The Ediacaran succession stratigraphically overlies Marinoan glaciogenic strata of the Ice Brook Formation and the informal Ravensthroat cap carbonate (James et al., 2001; Macdonald et al., 2013, 2018; Moynihan et al., 2019), which has been recently formalized as the Cliff Creek Formation (Busch et al., 2021). The Cliff Creek Formation is succeeded by a ~400 m-thick shale-dominated succession known as the Sheepbed Formation (Figure 2). In proximal areas of the Goz/Corn Creek region, the Sheepbed Formation is capped by ~100 m of recrystallized

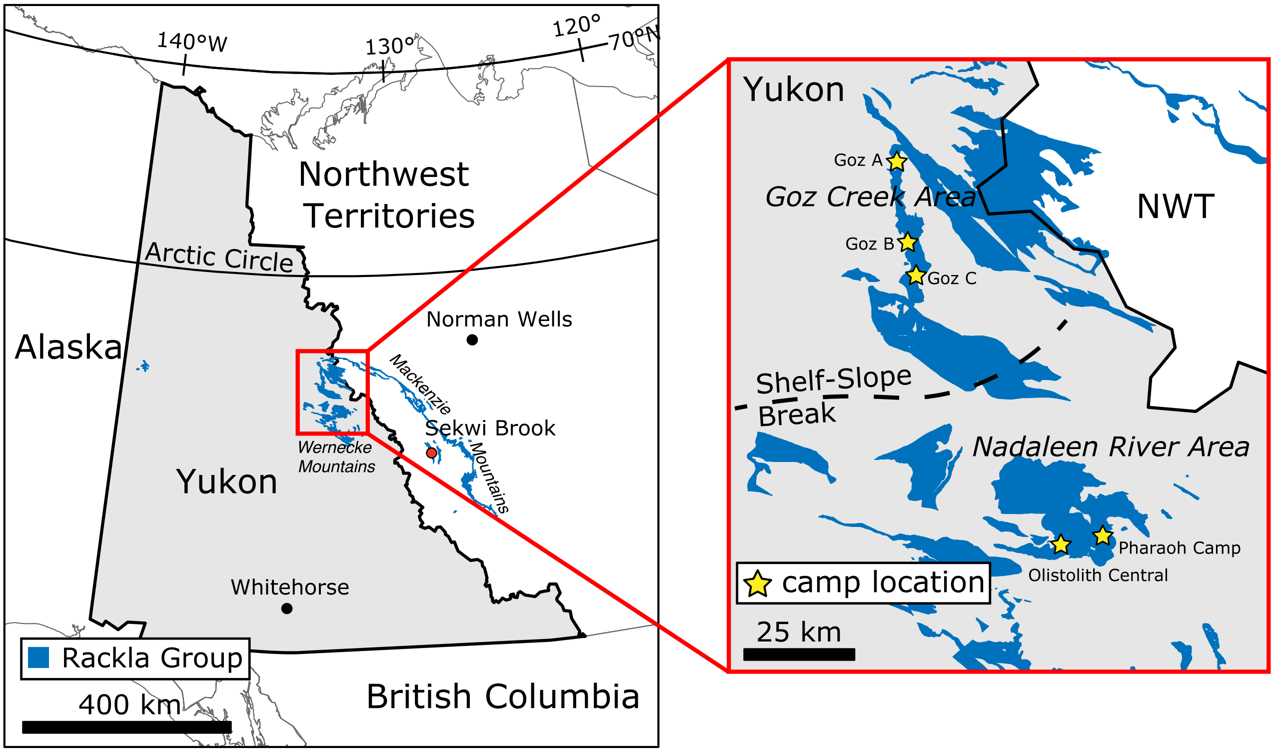

FIGURE 1 Location map. Study locations in the Goz/Corn Creek and Nadaleen River regions of the Wernecke Mountains, Yukon, Canada, with towns shown as black dots. The Sekwi Brook locality is another Ediacaran locality from the Rackla Group in the Mackenzie Mountains. Inset map: Shelf-slope transect from shallow-water facies at Goz A to offshore facies at Goz B-C, before moving into slope deposits found at Pharaoh and Olistolith Central camps in the Nadaleen River Area. Ediacaran strata in the Goz D region may have been translated into the region by later strike-slip faulting (see Busch et al., 2023). Figure adapted from Busch et al. (2023) and Moynihan et al. (2019).

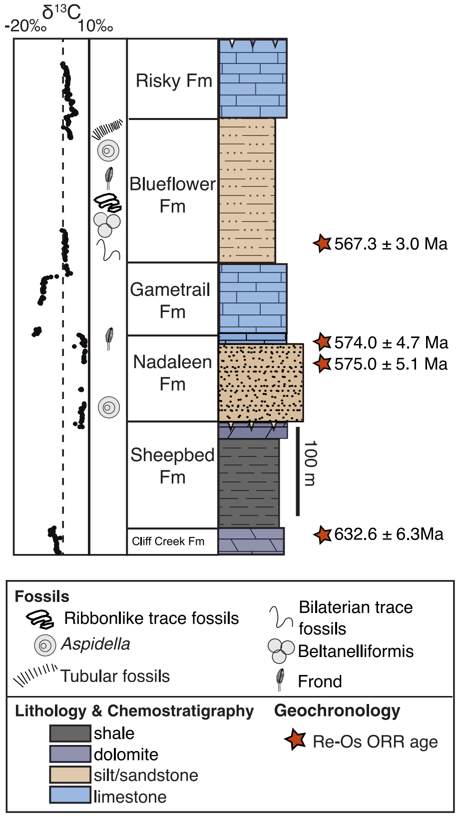

FIGURE 2 Stratigraphy of the Ediacaran Rackla Group. Generalized stratigraphy of the Ediacaran Rackla Group in NW Canada (following Busch et al., 2021; Moynihan et al., 2019; Rooney et al., 2020). Simplified carbonate carbon isotope profile denotes the Shuram carbon isotope excursion (CIE) within the Gametrail Formation (adapted from Rooney et al. (2020)). Paleontological information summarizes known fossils in the Nadaleen and Blueflower formations in Yukon (Wernecke Mountains); fossil data from these formations in the Northwest Territories (Sekwi Brook) can be found in Carbone et al. (2015), Narbonne & Aitken (1990), Narbonne (1994), Narbonne et al. (2014). Note fossils are depicted at the formational level and not in exact stratigraphic placement. The "sub-Cambrian" unconformity exists at the top of the Risky Formation, while the Ediacaran-Cambrian boundary is slightly higher in the Ingta Formation or the lacunae of the unconformity depending on the position in the basin. Re-Os organic-rich rock (ORR) geochronological and carbon isotopic data adapted from Rooney et al. (2015, 2020).

dolostone. In some areas, this carbonate has been identified as the Gametrail Formation (Narbonne, 2005; Pyle et al., 2004), but recent work suggested it rests gradationally upon the Sheepbed Formation and is referred to informally as the "Sheepbed carbonate" (Busch et al., 2023; Macdonald et al., 2013). At the shallowest-water Goz A section (Figure 5), the Sheepbed carbonate is capped by a subaerial karstic unconformity and overlain by interbedded shale, sandstone, and carbonate of the Nadaleen Formation (Macdonald et al., 2013) (note the Nadaleen Formation was previously referred to as the "June Beds" by Macdonald et al. (2013) before its formalization by Moynihan et al. (2019)). In the deeper-water deposits of the Nadaleen River area, the Nadaleen Formation has been divided into the informal lower carbonate, heterolithic, upper carbonate, black shale, and green siliciclastic members (Moynihan et al., 2019). The sedimentology and depositional setting of the Nadaleen Formation are key to understanding the paleoenvironmental setting of the earliest Avalon assemblage fossils in NW Canada and are discussed at length below.

The Nadaleen Formation is overlain by dolostone and limestone of the Gametrail Formation (Figure 2), which records the Shuram CIE (Busch et al., 2022, 2023; Macdonald et al., 2013; Moynihan et al., 2019). Above the Gametrail Formation, the terminal Ediacaran is recorded by the Blueflower and Risky/Algae formations (Figure 2). In shallow-water settings, the Blueflower Formation is predominantly composed of siliciclastic-dominated strata with local sandy carbonate facies. In deep-water settings, the Blueflower is subdivided into three informal members (Moynihan et al., 2019; Pyle et al., 2004). The lower carbonate member is a mixed carbonate-siliciclastic interval, the middle member is exclusively siliciclastic, comprising rhythmically bedded mudstone, siltstone, and quartz arenite, and the upper member is composed of heterolithic fine- and coarse-grained siliciclastic strata. Busch et al. (2023) recently proposed that the lower member of the Blueflower Formation should instead be included with the Gametrail Formation. In shallow-water settings, the top of the Rackla Group is marked by the dolostone-dominated Risky Formation, while in deeper-water settings this unit is dominated by limestone and dolostone of the Algae Formation (Cecile, 2000; Moynihan et al., 2019). A "sub-Cambrian" unconformity locally removed the Ediacaran-Cambrian boundary and separates the Risky/Algae formations from the overlying lower Cambrian shale-dominated Ingta and Narchilla formations (Nowlan et al., 1985; Pyle et al., 2006).

In the shallow-water deposits of the Goz/Corn Creek area, the paleontology of the Ediacaran succession has been studied for decades, albeit at a reconnaissance level (Hofmann et al., 1983; Narbonne & Hofmann, 1987). No body or trace fossils have been recovered to date in the Sheepbed, Nadaleen, or Gametrail formations, but the Blueflower Formation contains documented occurrences of the Ediacaran hold-fast disc *Aspidella*, an unnamed frond specimen, as well as the colonial *Beltanelliformis* (Hofmann et al., 1983; Narbonne & Hofmann, 1987; Pyle et al., 2004). The upper Blueflower Formation also contains simple trace fossils (*Helminthoidichnites*, *Planolites*, *Helminthopsis*) (Narbonne & Hofmann, 1987; Pyle et al., 2004). In contrast, the paleontology of the deep-water Nadaleen area was largely unexplored prior to this study. Moynihan et al. (2019) figured a single *Aspidella* specimen from the heterolithic member of the Nadaleen Formation and reported the simple trace fossils *Planolites* and *Helminthoidichnites* in the middle member of the Blueflower Formation. Thus, while the Goz area records well-preserved fossils in the Blueflower Formation, neither the Ediacaran paleontology of the deeper-water Nadaleen River area nor the suitability of unfossiliferous shallow-water Nadaleen Formation strata in the Goz area for preserving fossils have ever been fully examined.

Correlative Rackla Group strata in the Mackenzie Mountains (Northwest Territories) are located to the east and south of the

Wernecke Mountains (Figure 1). The best studied of these strata occurs in the Sekwi Brook area, where much of the succession was deposited in deep-water slope to shelf margin settings (Aitken, 1989; Dalrymple & Narbonne, 1996). The Nadaleen Formation at Sekwi Brook is composed of channelized carbonate-clast conglomerate and interbedded sandstone, siltstone, mudstone, and lime mudstone that suggest persistent low-energy slope sedimentation (Dalrymple & Narbonne, 1996) (note these strata were referred to as the Sheepbed Formation in previous studies but are now assigned to the Nadaleen Formation (Macdonald et al., 2013; Moynihan et al., 2019)). A diversity of Ediacaran fossils are found in the deep-water Nadaleen Formation at Sekwi Brook, preserved both on the base of turbidite beds but also intrastratally within sandstone layers (Narbonne et al., 2014). Taxa include *Aspidella* and fronds like *Charniodiscus*, *Charnia*, *Beothukis*, and *Primocandelabrum* (Narbonne et al., 2014). The overlying Gametrail Formation is locally composed of ~300 m of predominantly unfossiliferous thick-bedded dolostone with abundant carbonate rudstone (Aitken, 1989; Macdonald et al., 2013). This is followed by the Blueflower Formation, which is divided into a lower carbonate-dominated member (~300 m thick) and an upper siliciclastic-dominated member (~280 m thick). The lower member overlies the Gametrail Formation gradationally and is composed of ribbon-bedded micritic limestone and lesser beds of sandy limestone, while the upper member is predominantly composed of shale with minor sandstone (MacNaughton et al., 2000). The upper member of the Blueflower Formation records a shallowing-upward trend into offshore to lower shoreface settings (Carbone et al., 2015). The upper Blueflower Formation contains simple Ediacaran trace fossils (*Helminthoidichnites*, *Planolites*, *Helminthopsis*) (Carbone & Narbonne, 2014) and the body fossils *Aspidella*, *Windermeria*, and the tubular forms *Sekwitubulus* and *Annulatubus* (Carbone et al., 2015; Hofmann, 1981; Narbonne, 1994; Narbonne & Aitken, 1990), all of which are characteristic of the terminal Ediacaran Nama assemblage (Schiffbauer et al., 2016).

In contrast to the well-studied Ediacaran paleontology of the deep marine Sekwi Brook area, the paleontology of shallow-water Rackla Group strata exposed to the north and east in the Mackenzie Mountains is relatively poorly known. This is due in part to ambiguity regarding how strata above the Ravensthroat and Sheepbed formations—which are regionally referred to as the Backbone Ranges Formation—correlate with strata in the Sekwi Brook area and the Wernecke Mountains (e.g., Macdonald et al., 2013; MacNaughton et al., 2008). Recently, Geological Survey of Canada mapping projects have revealed Ediacaran body fossils in proximal areas at a stratigraphic position equivalent to the upper Blueflower Formation (MacNaughton, 2020; MacNaughton & Fallas, 2021; MacNaughton et al., 2018). Thus, although our reading of the Ediacaran paleontological record in the Mackenzie Mountains outside Sekwi Brook remains hindered by stratigraphic uncertainty (and extremely limited search efforts), the known pattern is consistent with that from the Wernecke Mountains. Specifically, Ediacaran body fossils are present in both the Nadaleen and Blueflower formations at the deep-water Sekwi Brook site and body fossils are recovered from the "Blueflower equivalent" in proximal sites, with no known fossils below that stratigraphic level in shallow water settings.

2 | METHODS

A paleontological and taphonomic investigation of the Nadaleen and Blueflower formations was conducted in the summers of 2017 and 2018 along a transect of informally named camps Goz A, Goz B, Goz C, Goz D (following the nomenclature of Narbonne & Hofmann, 1987; Pyle et al., 2004), Pharaoh, and Olistolith Central (Figures 1, 3 and 4). While previous studies in this region have included stratigraphic sections from Goz D in such transects, it has recently been recognized that this structural panel exhibits anomalous subsidence patterns and was likely transported to its current location via Mesozoic–Cenozoic strike-slip displacement (Busch et al., 2023). We note here that the paleobiological data from that camp are consistent with the pattern along the north–south transect from the Goz/Corn Creek to the Nadaleen River areas. At each camp, the entire Ediacaran succession was measured (time and exposure permitting) and investigated for both fossil occurrences and facies amenable to preservation. To test the likelihood of Ediacaran fossils occurring in shallow-water facies of the Nadaleen Formation, we evaluated two metrics common to stratigraphic paleobiology: 1. search intensity; and 2. taphonomic and sedimentologic preservation potential, including abundance of microbial mat structures and paleoenvironmental conditions analogous to other shallow-water Ediacaran localities.

3 | RESULTS

3.1 | Sedimentology and lithostratigraphy of the Nadaleen Formation across the Goz/Corn Creek - Nadaleen River transect

3.1.1 | Goz A-C

Although it has been previously recognized that Ediacaran units deepen from north to south along the Goz/Corn Creek-Nadaleen River transect (Busch et al., 2022, 2023; Macdonald et al., 2013; Pyle et al., 2004) (Figures 1, 3 and 4), there has been no detailed sedimentological and paleoenvironmental analyses of the Nadaleen Formation along this transect. At the northernmost camp, Goz A, the Nadaleen Formation is ~50 m thick and overlies the informal Sheepbed carbonate above a prominent karstic unconformity (Macdonald et al., 2013). The basalmost Nadaleen Formation strata consist of ~15 m of lenticular to planar, coarse-grained, trough cross-bedded quartz arenite which were deposited on an undulatory surface above an irregular paleokarst horizon. Above this, coarse- to fine-grained trough cross-bedded quartz arenite horizons are intercalated with vuggy and recrystallized dolograinstone or dolopackstone strata, some of which host relict-coated grains. At times, these

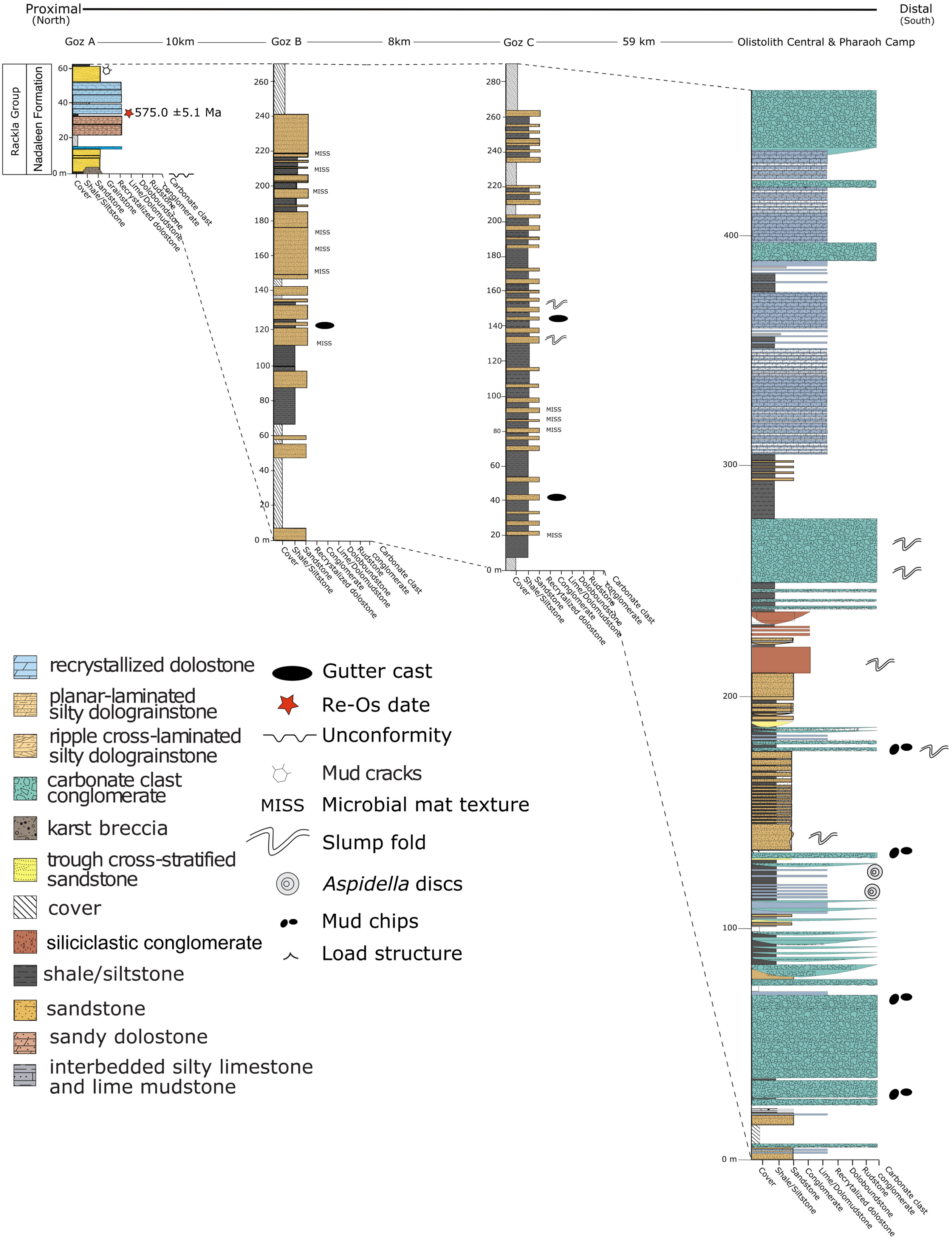

FIGURE 3 Stratigraphic fence diagram of the Nadaleen Formation along the Goz/Corn Creek-Nadaleen River transect. The figure shows correlation of the Nadaleen Formation from shallow-water facies of the Goz/Corn Creek area into slope facies in the Nadaleen River area. Stratigraphic column in the Nadaleen River area adapted from Moynihan et al. (2019). *Aspidella* fossils have been recovered from the deep-water heterolithic member in both the Olistolith Central and Pharaoh Camp localities in the Nadaleen region. See text for more detail on the sedimentological observations.

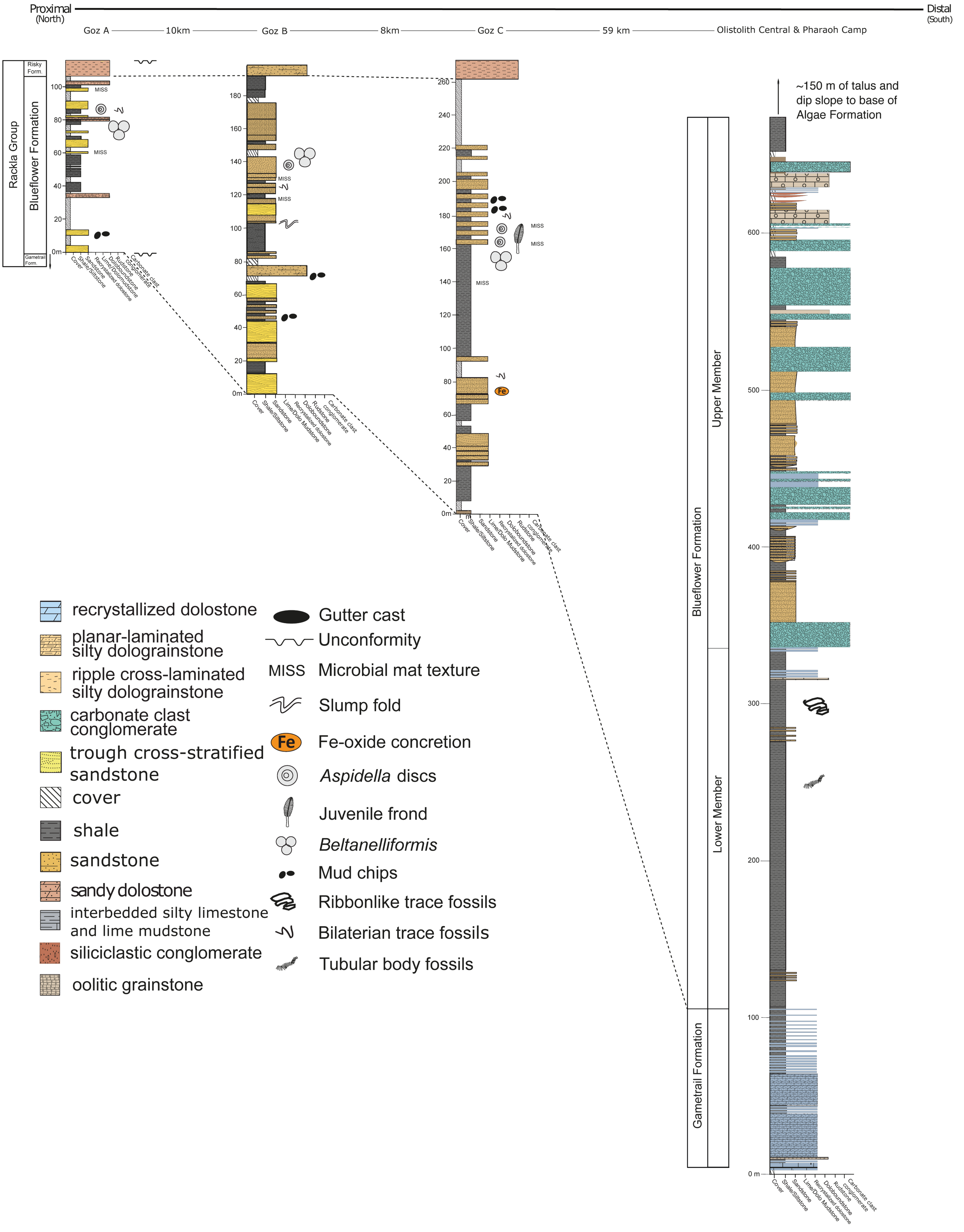

FIGURE 4 Stratigraphic fence diagram of the Blueflower Formation along the Goz/Corn Creek-Nadaleen River transect. The figure shows correlation of the Blueflower Formation from shallow-water facies of the Goz/Corn Creek area into slope facies in the Nadaleen River area. Stratigraphic position of Blueflower fossils in the Nadaleen River area is approximate as these fossils were found in float.

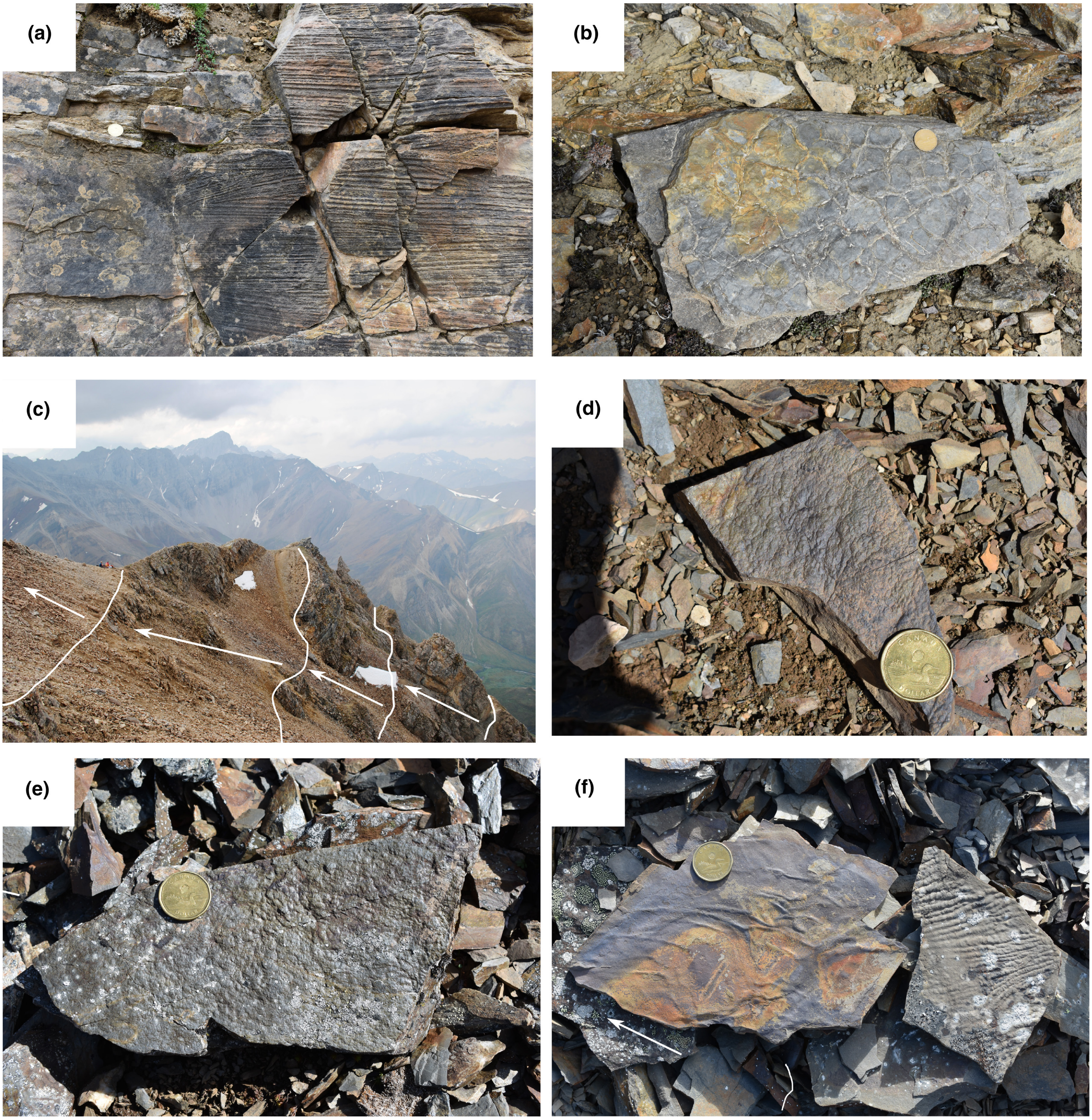

FIGURE 5 Shallow-water sedimentary facies of the Nadaleen Formation. Shelf facies of the Nadaleen Formation at Goz A display clear evidence for shallow-water marine sedimentation, including abundant trough cross-stratification in sandy dolograinstone facies (a) and subaerial exposure in the form of desiccation cracks (b). View looking south at distinct shoaling-upwards parasequences in the uppermost Nadaleen Formation at Goz A. Each parasequence consists of a basal mudstone or siltstone interval capped by a package of cross-bedded oolitic dolostone and/or dolomitic sandstone. Note people for scale in the uppermost parasequence (c). These strata also display a diversity of microbial mat textures, ranging from *Kinneyia*-type wrinkle structures (d) to clotted-type textured organic surfaces (e) and pucker-type textures in (f) (terminology after Gehling and Droser (2009)). Canadian coin for scale is 26.5 mm.

carbonate strata transition into mixed sandy dolostone and dolomitic sandstone (Figure 5a) with coarse-grained sparry cement. Above these basal strata are distinct m- to decameter-thick parasequences consisting of (in ascending order) thin-bedded shale and sandstone overlain by trough cross-bedded quartz arenite or recrystallized dolograinstone (Macdonald et al., 2013; Pyle et al., 2004). The Nadaleen Formation at Goz A is capped by a subaerial exposure surface, which is indicated by abundant desiccation cracks (Figure 5b).

To the south at Goz B, shelf facies of the Nadaleen Formation expand abruptly to 280 m thick (Figure 3). Here, the Nadaleen

Formation rests on a ~10-m-thick package of clast-supported rudstone/breccia with a dolomite-cemented sandy matrix. This rudstone/breccia interval likely represents the local equivalent of the Sheepbed carbonate and may record redeposition of carbonate material sourced from karsted portions of the more proximal Sheepbed carbonate observed at Goz A. The basal Nadaleen Formation here is composed of fissile shale interbedded with thin-bedded limestone and medium- to fine-grained quartz arenite. These mixed lithologies continue for ~50 m before another ~3-m-thick clast-supported rudstone/breccia unit with tabular limestone clasts. These strata are succeeded by ~50 m of poorly outcropping shale that terminates with another carbonate-clast rudstone with a sandy matrix. The uppermost Nadaleen Formation at Goz B is dominated by interbedded thinly laminated grey-green siltstone and fine-grained quartz arenite below the contact with the Gametrail Formation. The sandstone beds record abundant microbial mat structures that display symmetrical and asymmetrical ripples and gutter casts. Swaley cross-stratification is present in isolated beds of fine-grained sandstone.

At Goz C, the basal contact between the Nadaleen Formation and the underlying Sheepbed Formation is not exposed. The observable Nadaleen Formation is locally ~300 m thick, and the base is primarily composed of blue-grey thin-bedded sandy siltstone with planar lamination. Rarely, there are tabular beds of fine-grained quartz arenite which locally preserve microbial mat structures. At ~60 m in the measured section, an interval of fine-grained sublitharenite preserves symmetrical ripples and gutter casts. The remainder of the section primarily follows this same lithological suite with intervals of blue-grey siltstone interrupted by fine- to coarse-grained quartz arenite beds that display abundant microbially induced sedimentary structures (MISS) and occasional gutter casts and slump folds (Figures 3 and 5).

3.1.2 | Nadaleen River

Farther south, the type Nadaleen Formation in the Nadaleen River area expands to >800 m thick (Figure 3). Here, the ~60 m-thick lower carbonate member (Moynihan et al., 2019) is composed of carbonate-clast rudstone interbedded with grainstone and matrix-supported conglomerate with oolitic limestone clasts. This most likely represents a deep-water equivalent to the Sheepbed carbonate, similar to that documented at Goz B. Above this, the heterolithic member (Moynihan et al., 2019) is composed of a heterogeneous package of normal-graded sandstone, shale, limestone, and conglomerate. Mass transport deposits occur widely within these strata, with local rafting and imbrication of slope-derived mudstone clasts with prominent soft-sediment deformation (Figure 6c). Above the heterolithic member is the upper carbonate member, which is composed of interbedded calcareous shale and thin-bedded limestone with partial Bouma sequences. The top of the upper carbonate member is made up of a thick rudstone unit that is then overlain by the black shale member. The lower portion of this unit is composed of homogenous black shale, while the upper portion is dominated by interbedded sandstone and shale. The uppermost Nadaleen Formation is composed of the green siliciclastic member, which is dominated by green-grey shale and siltstone with occasional graded sandstone beds, interpreted to be upper slope turbidites (Moynihan et al., 2019).

3.2 | "Paleontology" of the shallow-water Nadaleen Formation

Our field observations, as well as previous field investigations (Busch et al., 2023; Hofmann et al., 1983; Macdonald et al., 2013; Narbonne & Hofmann, 1987; Pyle et al., 2004), failed to find shallow-water fossils in the Nadaleen Formation from the Goz/Corn Creek area—the critical question is whether this is due to lack of searching, lack of amenable preservation, or that the organisms were simply not living there. Regarding search effort, our research group spent more than 90 person days in the Goz area camps, with much time spent specifically aiming to find fossils in the Nadaleen Formation. Prior to this, researchers from Harvard and McGill universities spent an estimated 138 person days working on Ediacaran strata of the Goz/Corn Creek area (Macdonald et al., 2013), and researchers from Queen's University spent an estimated 72 person days in the region (Narbonne & Hofmann, 1987; Pyle et al., 2004). The Goz/Corn Creek area has also been studied extensively by the Geological Survey of Canada (Fritz et al., 1983; Nowlan et al., 1985), while researchers from Dartmouth and Virginia Tech universities subsequently worked in the area for 25 person days in 2022. During the 325 total person days documented, no body fossils were ever found. Considering the research efforts in the Goz/Corn Creek area and the number of experienced Ediacaran paleontologists and geologists who have worked there, we conclude that shallow-water Nadaleen Formation fossils are unlikely to be found.

The outstanding question then is whether the fossils would have been preserved had organisms been living there in the Ediacaran. Nadaleen Formation shallow-water facies from Goz B and C are both dominated by fine-grained siliciclastic strata displaying current-swept features indicative of deposition in offshore shelf conditions below fair-weather wave base (Pyle et al., 2004) (Figures 3 and 5c). This results in the generation of distinct bedding plane slabs on which Ediacaran fossils could potentially be preserved. Although such a factor as slab-forming strata may seem trivial, the lack of such slabs can render large portions of a stratigraphic column unamenable to fossil preservation (Sperling et al., 2016) and is an important consideration in placing confidence limits on where and when Ediacaran fossils appear in the record. Perhaps more importantly, many of these slabs at Goz A/B/C contain specific structures found in fossiliferous Ediacaran deposits elsewhere in the world. For example, these strata record a diversity of MISS features formed by layers of microbial mats on the sediment surface (Figure 5a,d–f), which are also common in the Ediacaran of South Australia (Tarhan et al., 2017). These mats are a critical component in "Flinders style" preservation (sensu Narbonne, 2005) of White Sea biota in shelf environments

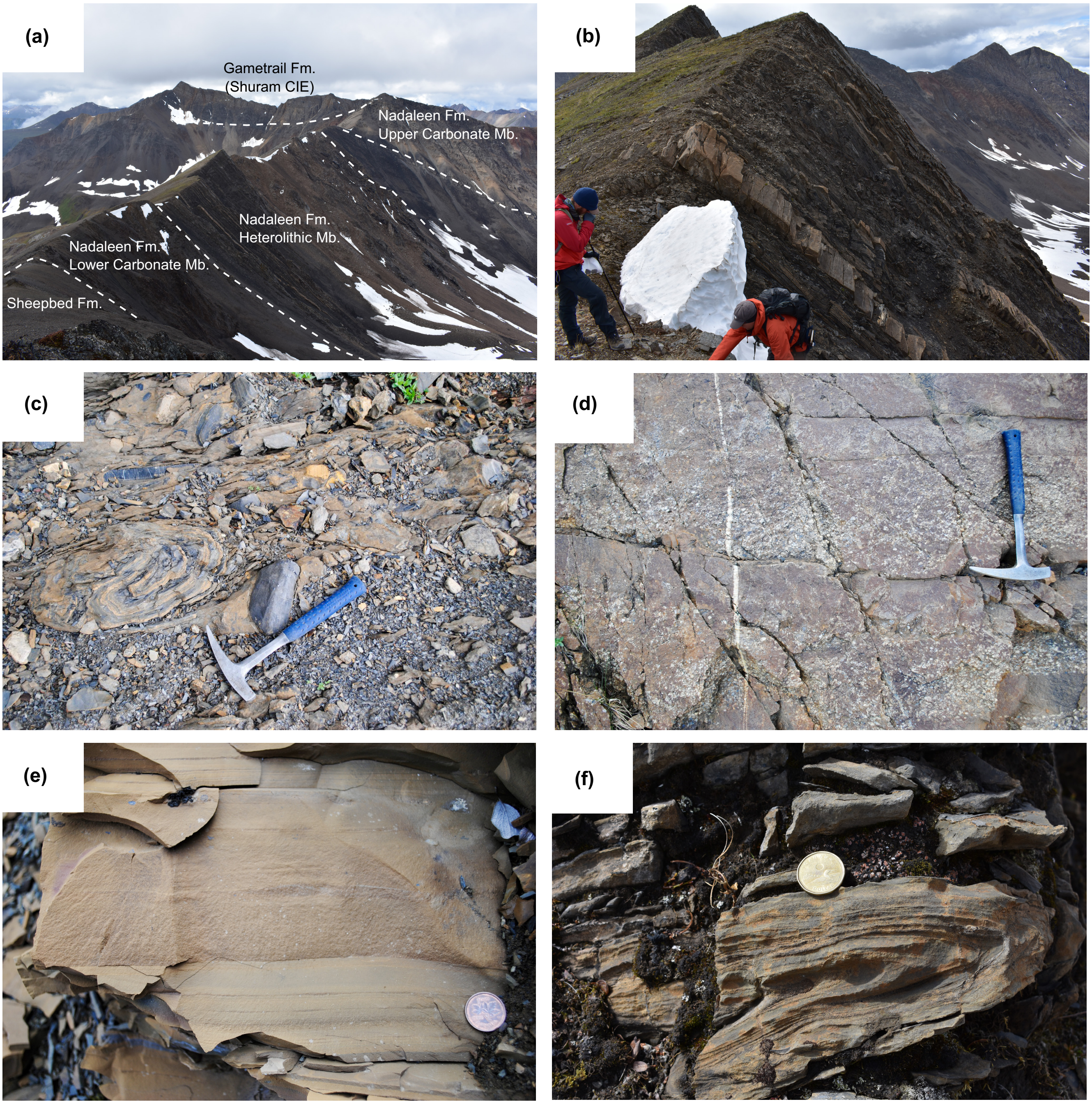

FIGURE 6 Deep-water sedimentary facies of the Nadaleen Formation. (a) Well-exposed Ediacaran strata in the Nadaleen River area (Pharaoh Camp), displaying a deep-water succession from black shale of the Sheepbed Formation (lower left) into the various mappable members of the Nadaleen Formation above. The ridgeline at the top of the frame is cliff-forming carbonates of the Gametrail Formation. (b) Well-preserved turbidite sequences within the fossiliferous heterolithic member of the Nadaleen Formation. Note: Localized faulting can be seen in the background by the displacement of the thick structureless sandstone bed. (c) Polymictic matrix-supported boulder conglomerate with intrabasinal shelf- and slope-derived carbonate clasts, as well as slump-folded mudstone and sandstone derived from underlying strata, in the heterolithic member of the Nadaleen Formation at the type section. These mass transport deposits indicate an active portion of the slope or basin-floor submarine fan where coarser-grained material was being transported in diverse sediment gravity flows. (d) Polymictic graded conglomerate beds from the Nadaleen River area at Pharaoh Camp are indicative of mass transport. Rock hammer for scale. (e) Thin-bedded turbidites displaying normal grading from the same Pharaoh Camp locality. Canadian penny for scale. (f) Fold structure at Pharaoh Camp, further evidence of significant soft-sediment deformation induced by slumping. Canadian coin for scale is 26.5 mm.

in Australia and Russia, as they both prevent erosion and enhance the preservation of soft tissues by sealing buried organisms between layers of sand (Darroch et al., 2012; Gehling, 1999; Gehling & Droser, 2009; Slagter et al., 2022). Furthermore, in the absence of widespread deep-burrowing animals, microbial mats in the Ediacaran may have also played a key ecological role for sessile

Ediacara organisms by bounding the upper few centimeters of benthic sediment and providing a cohesive substrate integral to the lifestyle of many organisms (Droser et al., 2022; Laflamme et al., 2012; Seilacher, 1999; Tarhan et al., 2022).

Previous work has shown some, but not all, shallow-water Ediacaran taxa are capable of living in all Nadaleen Formation facies present in the Goz Creek area. For example, in South Australia, classic taxa of the White Sea biota, including *Dickinsonia* and *Parvancorina*, are preserved in sandstone-dominated strata across wave base, as well as delta front deposits, that resemble some facies at Goz B-C (Gehling & Droser, 2013; McMahon et al., 2020). *Aspidella* also demonstrates a similarly cosmopolitan environmental distribution in South Australia, but with even higher abundance (Gehling & Droser, 2013). While some White Sea fauna certainly lived in restricted environments, the diversity of facies and amenable taphonomic conditions across the shelfal portions of the Nadaleen Formation in the Goz Creek area, combined with the considerable search intensity undertaken over multiple decades, makes the lack of a single fossil discovery extraordinary when compared to younger Ediacaran basins.

3.3 | Paleontology of the deep-marine Nadaleen Formation

We describe here newly discovered *Aspidella* discoidal holdfasts including convex relief morphotypes *Kullingia* sp. (Figure 7a) and

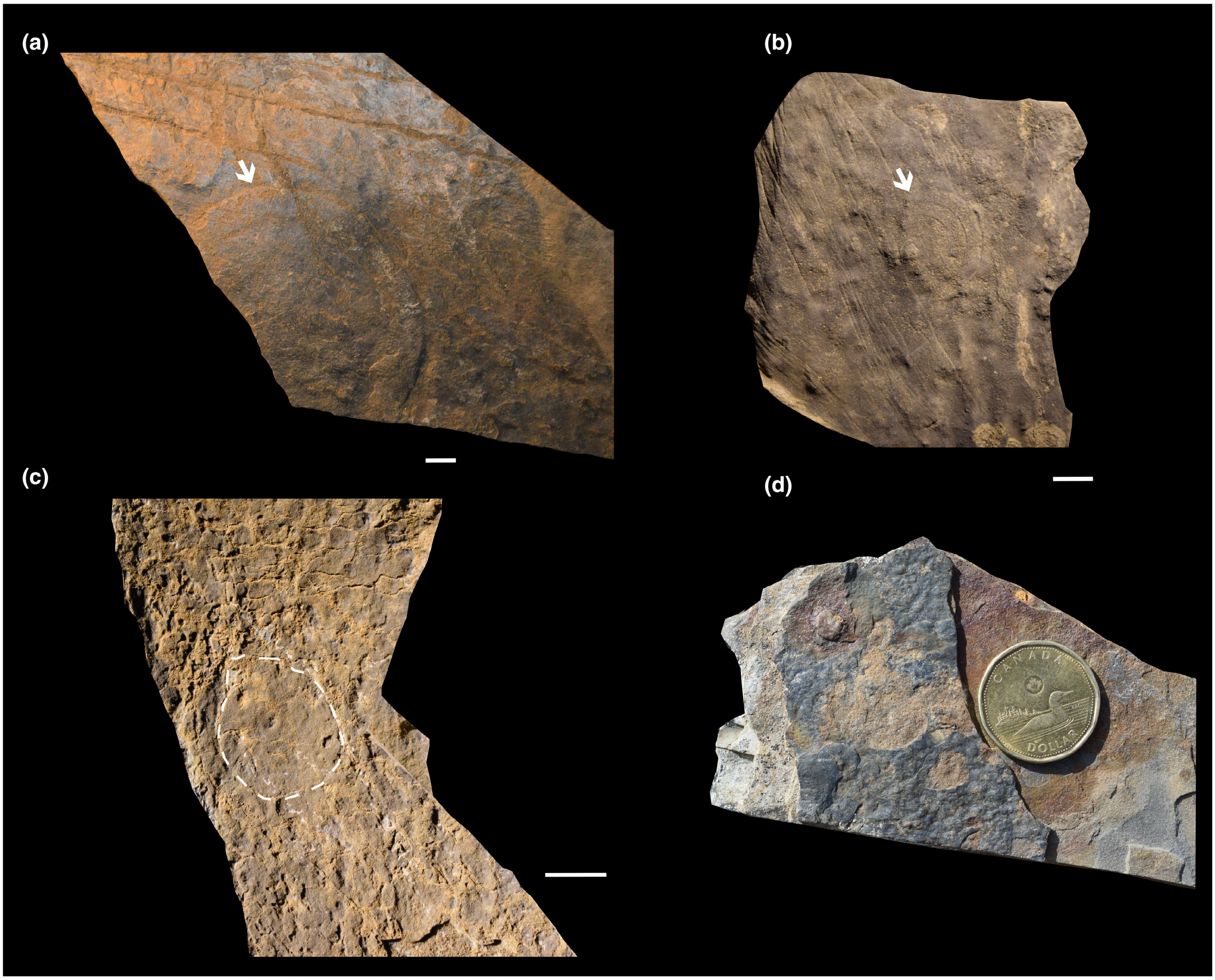

FIGURE 7 Deep-water fossils of the Nadaleen Formation in the Nadaleen River area. (a) *Kullingia* sp. morphotype disc in positive epirelief discovered at Pharaoh camp, and (b) Single *Aspidella* displaying prominent central boss with several sets of rings surrounding it recovered from Olistolith Central, similar to the *Cyclomedusa* sp. morphotype as figured in Narbonne & Hofmann (1987). (c) Flat, annulate *Aspidella* displaying a range of taphonomic quality with varying features preserved, also recovered from Olistolith Central. Most similar to the *Spriggia* sp. morphotype from Gehling et al. (2000) and Narbonne & Hofmann (1987). The range in preservation quality is likely due to the uprooting of a once-attached frond due to currents that eventually resulted in the burial of the discs, for instance in (d) only the central boss of an *Aspidella* is preserved on a microbial mat from the heterolithic member of the Nadaleen Formation at Pharaoh Camp (top left corner of slab). Scale bars = 1 cm.

Cyclomedusa sp. (Figure 7b), the flat relief morphotypes *Spriggia* sp. (Figure 7c), and less well—preserved discs that retain a central boss (Figure 7d) (nomenclature follows that of Gehling et al., 2000; Narbonne & Hofmann, 1987). These fossils have been recovered from the heterolithic member of the Nadaleen Formation in multiple deep-water slope localities of the Nadaleen River area (Pharaoh Camp and Olistolith Central). Like the fossiliferous deep-water sandstone deposits at Sekwi Brook (Mackenzie Mountains), deep-water fossils in the Wernecke Mountains are predominantly recorded through "Fermeuse-style" preservation, either in positive hyporelief on the soles of sharp-based turbidites or in negative epirelief on the top of the underlying bed (Narbonne, 2005). In this taphonomic mode, hold-fast discs and trace fossils are preferentially preserved due to their semi-infaunal position during life. In contrast, many Sekwi Brook taxa are also preserved within sandstone beds, referred to as intrastratal or "Nama style" preservation (Narbonne, 2005), as opposed to just preservation of the bed surface ("Fermeuse"). Most likely the higher energy slope setting of the Nadaleen River area is not amenable to this additional preservational style. Despite the predominance of high-energy flow regimes, some intermittent *Aspidella* fossils do record partial "Nama-style" preservation in lower-energy turbidites. For instance, the *Aspidella* disc shown in Figure 7b shows preservation of multiple concentric rings across multiple fine layers of sediment, and another *Aspidella* in this bed possibly records a poorly preserved frond. Despite these instances, the overall preservational regime limits the extent to which frond diversity can be determined. *Aspidella* themselves are a shared element of all fronds, but despite impressive morphological variation, they cannot be used to identify the taxonomy of the attached frond (Burzynski & Narbonne, 2015). Nonetheless, although the general taphonomic setting of the deep-water Nadaleen Formation in the Nadaleen River area does not allow for the preservation and documentation of diverse fronds as at Sekwi Brook, their occurrence across multiple localities unequivocally confirms the presence of deep-water Avalon assemblage fronds stratigraphically beneath the Shuram CIE.

3.4 | Paleontology of the Blueflower Formation

In contrast to the paleontological pattern observed in the Nadaleen Formation, the Blueflower Formation records a diversity of trace and body fossils in both shelf and slope facies. In shelf facies at Goz A and Goz B, numerous new specimens of convex epirelief *Aspidella* discs were recovered (Figure 8a displaying similarities to *Tirasiana* sp. morphotype, and Figure 8b comparable to the *Cyclomedusa* sp. morphotype figured in Narbonne & Hofmann (1987)). In addition, colonial aggregations of *Beltanelliformis* (Figure 8c, with noted similarity to the *Beltanelliformis brunsae* specimens figured in Narbonne & Hofmann, (1987)) were also found. The discovery of these fossils is consistent with previous finds at these localities (Narbonne & Hofmann, 1987; Pyle et al., 2004). Several juvenile fronds were also discovered for the first time in the region (Figure 8d), and due to the presence of an external stalk they could represent the genera *Arborea*, *Charniodiscus*, or *Trepassia*. Adult *Charniodiscus* specimens have been found in NW Canada previously at Sekwi Brook (Narbonne et al., 2014), and all are present at Mistaken Point, Newfoundland (Laflamme & Narbonne, 2008; Liu et al., 2012). One frond preserves a circular depression at its base which likely represents the external stalk passing through the bedding plane, while the petaloidium show differential preservation indicative of the dynamic burial that preserved these fronds. At a finer scale, secondary branches moving outwards from the central stalk are also visible, although the silt and sand grain-size are too large to see higher orders of self-similar fractal morphology needed to accurately assign a genus-level taxonomic designation.

In deep-water deposits of the lower Blueflower Formation at Olistolith Central, a new trace fossil we informally name *problematicum* was recovered with clear curve and looping behavior (Figure 8e). A variety of complex trace fossil have been previously recognized in NW Canada from the Blueflower Formation and the Cambrian Ingta Formation (Carbone & Narbonne, 2014; Pyle et al., 2004). This specimen requires important consideration, both due to its apparent size and its occurrence in deep-water settings. As this is a single specimen, we designate it as a *problematicum* until further specimens can be found that further elucidate the taxonomy.

Multiple specimens of a tubicolous organism were also discovered for the first time in the Blueflower Formation of the Nadaleen River area. These consist of annulated tubes preserved on the top of a microbial mat-covered slab (Figure 8f). At Sekwi Brook, multiple species of tubular body fossils have been described. These include the rigid *Sekwitubulus annularis* and flexible *Annulatubus flexuosus* (Carbone et al., 2015). The specimen discovered in the Nadaleen River area was highly flexible, implied by its ribbonlike

FIGURE 8 Shallow- and deep-water fossils of the Blueflower Formation. (a) Well-preserved *Aspidella* discs of the *Tirasiana* sp., (b) and *Cyclomedusa* sp. morphotypes preserved in sandy siltstone partings discovered from Goz B (morphotype nomenclature follows Narbonne & Hofmann (1987)). (c) Colonial aggregations referred to as *Beltanelliformis* recovered from Goz A. This taxon is found in the Blueflower Formation throughout NW Canada and commonly co-occurs with simple horizontal trace fossils such as *Planolites* and *Helminthoidichnites*. (d) Two well-preserved juvenile fronds with at least one order of branching were found at Goz B. (e) A newly discovered trace fossil we informally name *problematicum* from deep-water deposits of the Blueflower Formation at Olistolith Central in the Nadaleen River area. This large slab shows numerous visible impressions that are 0.5–1.5 cm in diameter and often overlap. This is a single specimen and thus any taxonomic interpretation will require further specimens to be found. (f) Ediacaran tubular fossils (arrows) recovered from deep-water deposits of the Blueflower Formation at Olistolith Central. Scale bar = 1 cm.

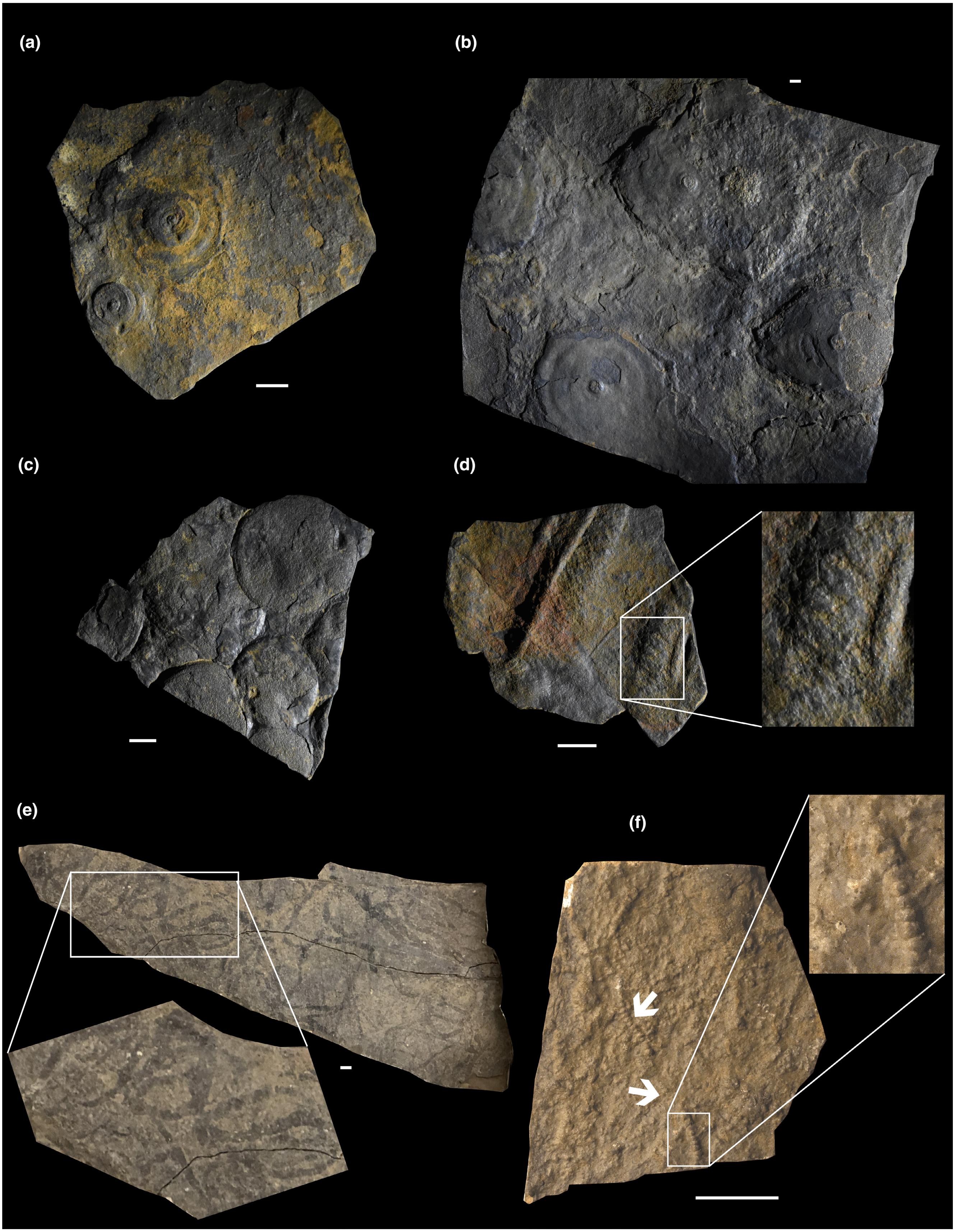
(a)
(b)
(c)
(d)
(e)
(f)

features (Figure 8f). This ribbonlike morphology is unlike a trace fossil, as the specimen clearly overlaps itself in multiple instances but does not cross-cut – implying the fossil was never bioturbating through sediment (Figure 8f above lower arrow). Furthermore, there are clearly preserved cylindrical (disc-shaped) transverse annulations, implying a three-dimensional bodyplan. The new Blueflower fossil is broadly like specimens recovered from the terminal Ediacaran Nama Group in Namibia, which have been tentatively assigned to the genus *Shaanxilithes ningqiangensis* (Darroch et al., 2016), although there are several critical differences. The specimen's annulated discs are far closer together than the Nama fossils and are therefore also somewhat different in gross morphology from the tubiculous fossils both in South China (Hua et al., 2000; Xing et al., 1984) and Namibia. Despite this taxonomic uncertainty, the new fossil discoveries highlight the presence of Ediacaran fossils in both shallow and deep-water depositional settings in the Blueflower Formation.

4 | DISCUSSION

4.1 | Paleoenvironmental interpretations of the Nadaleen Formation

Following subaerial exposure and erosion of the Sheepbed carbonate, the Nadaleen Formation at Goz A experienced an initial deepening into subtidal to supratidal settings within and above fair weather wave base. This is indicated by the predominance of trough cross-stratified sandstone, sandy dolostone, and coated grain grainstone, as well as the presence of distinct parasequences. The top of the Nadaleen Formation at Goz A also records evidence for another episode of subaerial exposure, indicating a consistent depositional setting within or above wave base. The presence of swaley cross-stratification in the Nadaleen Formation at Goz B is also an important paleoenvironmental indicator. Hummocky and swaley cross-stratification has been traditionally interpreted to result from oscillatory and combined flow conditions produced by storms between fair-weather and storm wave base between ~15 and 50 m water depths (Arnott, 1992; Duke, 1985). Evidence from the rock record supports this pattern, as swaley cross-stratification is often recorded overlying hummocky cross-stratification in shallowing-upward marine successions (Arnott, 1992).

The occurrence of gutter casts in the Nadaleen Formation at Goz B and C is also of note, as the fine-grained lithology and distal location of the Goz C camp relative to the shallow-water Goz A locality indicates a transition into a slightly deeper-water depositional setting. Gutter casts can occur in many depositional settings if there is significant erosional capacity (e.g., from deep-water sediment gravity flows to fluvial channel settings), although the location of the Nadaleen Formation at Goz C midway along the shelf-slope transect likely indicates a storm-generated source for these gutter cast deposits (Myrow, 1992). In the fine-grained sandstone intervals above these strata are several event beds with soft-sediment deformation features, such as shale rip-up clasts (Pyle et al., 2004; their Figure 6c, note that the basal member of the Blueflower Formation reported in that study is actually the Nadaleen Formation. For discussion see Macdonald et al., 2013). This is likely caused by rapid sedimentation and liquefaction as storm-generated currents interacted with the seafloor (Dalrymple, 1979; Jelby et al., 2020). These features in the Nadaleen Formation indicate that strata south of the subaerially exposed Goz A locality were likely deposited in a shallow shelfal environment between ~15 and 50 m of water depth under the influence of wave action (Arnott, 1992; Duke, 1985).

In contrast, the widespread presence of sediment gravity flow deposits, including turbidites and debrites, suggests that the fossiliferous heterolithic member of the Nadaleen Formation in the Nadaleen River area was likely deposited within a slope depositional environment (Moynihan et al., 2019). Based on these results, the shelf-slope break along the Rackla Group transect was likely present between Goz C and the Nadaleen River area during Nadaleen time. This indicates that all sections within the Nadaleen Formation north of Goz C were deposited at storm wave base and above, while sections to the south represent slope to basin-floor deposits. Using these paleoenvironmental interpretations, the occurrence of Ediacaran fossils exclusively in deep-water settings of the Nadaleen River area (and absence in the Goz/Corn Creek area) prior to the Shuram CIE represents the best sedimentological evidence supporting the deep-water (>200 m) evolution of Ediacaran organisms.

4.2 | The age for the Blueflower Formation and its importance for understanding global trends in Ediacaran biodiversity

New geochronological constraints on the age and duration of the Shuram CIE in the Gametrail Formation also place new temporal considerations on the age of the Blueflower Formation (Busch et al., 2023; Rooney et al., 2020). Traditionally this unit has been assigned a terminal Ediacaran age (<550 Ma) based on the complexity of its trace fossils and lack of older White Sea biota (Carbone et al., 2015). However, given the Shuram CIE is now known to terminate at ca. 564 Ma, much more of the White Sea assemblage time interval (ca. 560–550 Ma) could theoretically exist within the lower Blueflower Formation. A better understanding of the age range of the Blueflower Formation will be a critical addition to Ediacaran evolutionary history given the diversity of fossils found within this unit. For instance, the report of *Windermeria aitkeni* from upper Blueflower Formation strata in the Sekwi Brook area (Narbonne, 1994) has at one point been suggested to be a White Sea-style dickinsoniid. Beyond the uncertainty of *Windermeria*'s taxonomy, it also co-occurs locally alongside multiple tubular genera characteristic of the terminal Ediacaran Nama assemblage (Schiffbauer et al., 2016), *Aspidella*, and numerous trace fossils (Carbone et al., 2015; Carbone & Narbonne, 2014). If this specimen is not a dickinsoniid, this would relax available biostratigraphic age constraints and allow the upper part of the Blueflower Formation to reflect sedimentation during ca. 550–540 Ma Nama assemblage time. Thus, more work is needed to understand the affinity of *Windermeria*, as it would aid in understanding whether any biostratigraphic overlap exists for the White Sea and Nama biotas. Future geochronological efforts to constrain the age of the Blueflower Formation will therefore also have significant additional implications for Ediacaran biostratigraphy.

4.3 | Time versus water depth in the Avalon assemblage

There has been a long debate in the Ediacaran literature regarding the extent to which the three Ediacaran fossil assemblages represent a biostratigraphic succession, an environmentally controlled biotope (e.g., a reflection of water depth, paleohabitat, etc.), broad-scale preservational bias, or biogeography (discussed by Boag et al. (2016), Grazhdankin (2004), Gehling & Droser (2013), Narbonne (2005), Waggoner (2003)). Our newly discovered fossils from the Wernecke Mountains, in the context of the shelf-slope transect from Goz/Corn Creek to Nadaleen River, provide the first evidence that the origination of the Ediacara biota in deep-marine environments is a robust paleontological pattern when tested in a basin with appropriate and coeval shallow-water facies. Because this approach is based on an "absence of evidence," it could be refuted simply by finding shallow-water Ediacaran fossils that are older than ~565 Ma. While this straightforward test remains open, the environmental hypothesis has proven robust to the first stratigraphic paleobiological investigation, and all current published data support a paleoenvironmental control on the nature of the Avalon assemblage's appearance in the fossil record (Boag et al., 2016; Narbonne, 2005; Narbonne et al., 2014). However, there is also an important temporal component that could not previously be tested without robust geochronology. These Wernecke Mountains Avalon assemblage fossils occur several hundreds of meters below new Re-Os dates from whole-rock organic-rich mudstone beneath the Nadaleen-Gametrail Formation contact. Specifically, the Re-Os ages of 574.0 ± 4.7 and 575.0 ± 5.1 Ma stratigraphically above the fossils (Rooney et al., 2020) indicate that these new discoveries are among some of the oldest complex Ediacaran macrofossils in the record and that they are coeval within radiometric age uncertainties to ca. 574 Ma fronds in the Drook Formation of Newfoundland (Matthews et al., 2020; Pu et al., 2016; Rooney et al., 2020). Despite the analytical uncertainty on these ages individually, it is likely that all these fossils appeared in a relatively narrow window postdating the Gaskiers glaciation and preceding the Shuram CIE (Rooney et al., 2020) (Figure 9), and then remained in these deeper-water settings for a protracted period of time. Put differently, arguments for temporal versus environmental controls on the appearance of the Avalon assemblage are not mutually exclusive: the fossils are old *and* solely inhabited deep waters (Figure 10).

4.4 | The role of physiology in the origination of Ediacaran organisms

The hypothesis derived from other successions worldwide that the Ediacara biota first appeared in deep water is consistent with this stratigraphic paleobiological examination. Thus, it is worth considering possible environmental drivers for both the initial appearance of the Avalon assemblage in deeper waters and the radiation/appearance of Ediacaran organisms to shelfal environments in White Sea time. Although an environmental/ecological driver is not strictly required, both evolutionary events appear to involve multiple independent clades (e.g., frondose rangeomorphs and arboreomorphs, and possible metazoan cnidarians and sponges) following the same pattern (a polyphyletic radiation), pointing to an external environmental forcing rather than, for instance, a key innovation or genetic trigger in one clade (an adaptive radiation). Further, some of the same organisms (specifically *Aspidella*) are found in the Avalon assemblage in deep water and the White Sea assemblage in shallow water, suggesting this environmental shift was not due to wholesale replacement of one group of organisms with a given physiology by another. In Precambrian paleobiology much weight is given to the role of oxygen, and although oxygen is an important factor in controlling habitability for large multicellular eukaryotes (Cole, Mills, et al., 2020; Sperling et al., 2022), the role of environmental perturbations in governing where and when Ediacaran organisms evolved is likely to have been more complex than just redox changes alone. Sperling and Stockey (2018) used the metaphor of the "fire triangle" in discussing animal energetics and habitability, comprising the fuel (organic matter), oxygen, and heat (temperature) that are required to sustain a fire (in the metaphor) or as discussed here, life in ancient oceans. We will use this energetic framework in considering the role of environment in the early evolution of the Ediacara biota in deeper water.

Considering the environmental downsides of the deeper ocean discussed in the introduction (specifically, lower levels of food, oxygen, and light compared to shallower waters), it is likely that this setting provided a potential refugium for Avalon assemblage organisms against some detrimental oxygen, temperature, or food supply condition of the mid-Ediacaran marine system. Three hypotheses explored below are: (1) escape from high surface temperatures that caused hypoxic stress, (2) escape from high surface temperatures that resulted in high food demand, and (3) escape from surface temperature fluctuations that pushed organisms into hypoxic stress. Notably, all three of these hypotheses rely on an assumption of lower-than-modern levels of atmospheric oxygen in the Ediacaran, an idea that has strong empirical and modeling support even if the exact oxygen levels, and the exact timing of fluctuations, remain uncertain (Krause et al., 2022; Lu et al., 2018; Sperling, Wolock, et al., 2015; Stolper & Keller, 2018).

With respect to the first hypothesis, it is important to consider that environmental oxygen and temperature are synergistically linked via aerobic metabolism, since metabolic rates increase exponentially with temperature (Gillooly et al., 2001; Schulte, 2015). Consequently, at increased temperatures, organisms require

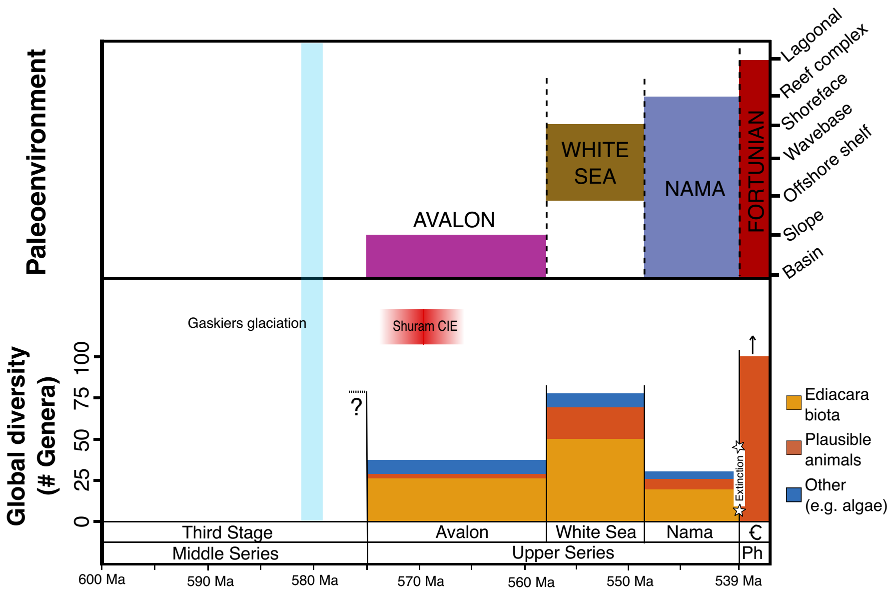

FIGURE 9 Paleoenvironmental habitats of Ediacara biota through time. (Top) Paleoenvironmental habitats occupied by Ediacara biota, including diverse frond groups and possible animals from the deep-water Avalon communities, shallow-water White Sea ecosystems made up of mobile bilaterians and Ediacara biota (note there are no known basinal occurrences of the White Sea biota, but also no known outcrops of that age that have received extensive study), and the terminal Ediacaran Nama interval made up of increasingly complex bilaterian trace fossils, tubicolous animals, early skeletonizing fauna, and depauperate groups of classical Ediacara biota. Data from Boag et al. (2016). (Bottom) Revised Ediacaran timescale showing trends in body-fossil diversity within a revised chronostratigraphic framework developed from new constraints on the Shuram CIE from Rooney et al. (2020). Proposed stage and series terms from Xiao et al. (2016). Ph, Phanerozoic, Є, Cambrian. Data from Muscente et al. (2018).

increasingly higher levels of oxygen to meet metabolic demand (Deutsch et al., 2015; Sperling et al., 2022; Stockey et al., 2021). With lower Ediacaran atmospheric oxygen levels, one possibility to explain the deep-water appearance of the Avalon assemblage is simply that the surface ocean was too hot for animal life. Note that temperatures required for this scenario need not be that extreme—there is little aerobic safety margin for elevated metabolic rates if atmospheric oxygen is low (Stockey et al., 2021). Given an oceanic temperature structure where deep waters are considerably cooler than the surface (see Figure 4 of Boag et al. (2018)) the deep ocean would certainly have provided a temperature refuge against elevated metabolic rates and consequent higher oxygen demand. Two lines of evidence, however, argue against this being the primary driver of the observed deep-sea origination hypothesis. First, even in a “hot” Earth system, temperatures at the poles are still generally equitable, and no shallow-water Avalon assemblage fossils have been found on the continents at presumed temperate/polar latitudes, such as Azania, Amazonia, Avalonia, Coats Land Block, Congo, Dronning Maud Land, Kalahari, and Rio de La Plata (noting that not all of these continents have appropriate aged sedimentary successions and/or well-constrained paleomagnetic data, and that Avalonia, the paleocontinent containing the deep-water Mistaken Point and Charnwood Forest assemblages, does not have shallow-water strata that are >567 Ma (pre-Shuram CIE) in age) (Evans et al., 2022; Matthews et al., 2020; Merdith et al., 2021; Rooney et al., 2020). Second, recent geochemical temperature records for the ca. 590–550 Ma period suggest that while the Shuram CIE interval itself may have been associated with substantial warming, the temperatures prior to and during the appearance of the Avalon assemblage were not actually that hot (Bergmann, Osburn, et al., 2022, in agreement with the worldwide occurrences of glaciogenic sedimentological evidence as seen in Hoffman and Li (2009) and Wang et al. (2023)). This is especially true when compared to other times in the Tonian or Cambro-Ordovician where much hotter tropical temperatures of ~35–45°C have been suggested (Bergmann, Boekelheide, et al., 2022; Goldberg et al., 2021; Hearing et al., 2018).

A second hypothesis to explain the deep-water appearance of the Avalon assemblage relates temperature to food demand. In essence, this is a similar argument as above, but concerning the other half of the highly simplified respiration reaction ($CH_2O + O_2 \Rightarrow CO_2 + H_2O$ + energy). In this second scenario, food supply is limiting, and so organisms seek cooler habitats to lower their energetic requirement (through lower metabolic rates) and thus lower their required food intake (note there are other effects on food and oxygen provisioning at cold temperatures that are not discussed here (see Boag et al., 2018; Simpson, 2021; Verberk et al., 2011; Woods et al., 2022)). Critically, recent geochemical data and modeling have suggested that if the Proterozoic Earth system was low in oxygen, it also likely had low primary productivity between 1% and 10% of modern levels (Derry, 2015; Laakso & Schrag, 2018; Ozaki et al., 2019; Reinhard et al., 2017; Sperling & Stockey, 2018). Low primary productivity likely occurred because anoxic and ferruginous conditions stripped phosphorus from the

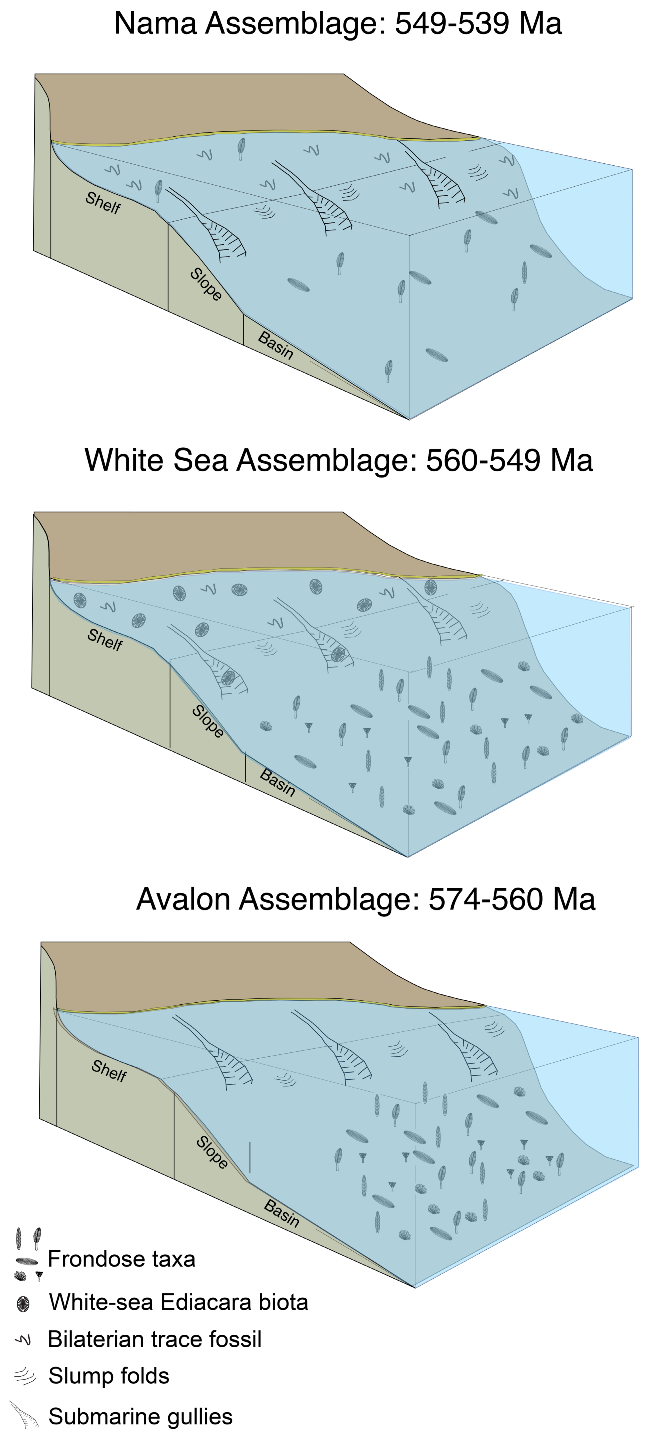

FIGURE 10 Block diagram of bathymetric evolution of the Ediacara biota. Block diagrams denote the successive evolution of Ediacaran habitat changes from bottom to top. During the deposition of the Avalon assemblage, global assemblages of frond species from Newfoundland, NW Canada, and England are restricted to slope and bathyal settings and are entirely absent from shallow-water facies. This previously known depth restriction is now supported by stratigraphic paleobiological study along the Goz-Nadaleen transect in the Wernecke Mountains. Transitioning into the White Sea interval, classical Ediacara biota (e.g., *Dickinsonia*, *Kimberella*) appear in shelf habitats, predominantly in South Australia and the White Sea area of Russia. Also occurring alongside these mobile organisms are emerging simple trace fossils. As noted in Figure 9, deep-water fossils in White Sea time are not known, but are drawn here schematically as they are unlikely to have been extirpated from this environment. The Nama assemblage occurs in the terminal Ediacaran and represents a dramatic reduction in the diversity of Ediacara fauna occurring in both shelf and slope environments. In comparison, trace fossil abundance and complexity increase significantly, alongside early skeletonizing animals and tubiculous body-fossils.

oceans (Derry, 2015; Reinhard et al., 2017), although the exact mechanism is not known with certainty. In any case, low primary productivity is likely a requirement for maintaining a low-oxygen Earth system, as high levels of primary productivity coupled with widespread reducing conditions would eventually result in large organic carbon burial and the oxygenation of the Earth system (Ozaki et al., 2019). Although these modeling efforts cited above are normally focused on a time-agnostic "mid-Proterozoic," low levels of shale total organic carbon contents through the Ediacaran (Sperling & Stockey, 2018) could be taken as empirical evidence for low productivity extending through that time interval. In this hypothetical Ediacaran world with limited food supply, one viable ecological strategy might be to limit metabolic demand. Recent studies of the ectothermic Greenland shark (a long-lived sluggish predator inhabiting polar regions) have demonstrated extremely low field metabolic rates and consequently low prey consumption requirements (Ste-Marie et al., 2022). In fact, their field metabolic rate is ~10–20 times lower than similarly sized bull sharks living in tropical habitats (Lear et al., 2020). It may simply be that the cold, deep sea was the only habitat in the middle Ediacaran where animals could depress their metabolic rates sufficiently to meet the limited available food supply, recognizing that the decrease in organismal food demand with depth must be sharper than the attenuation of food supply with depth. While this "Greenland shark" strategy may explain some of the paleontological pattern, it also cannot explain why Avalon assemblage organisms are not found in polar regions, which, given available temperature records (Bergmann, Osburn, et al., 2022) suggest that similarly cold temperatures to the deep sea (and concomitantly low metabolic rates) would also have been found at high latitudes. Again, uncertainties in Ediacaran paleogeographic reconstructions also confound this counterpoint.

A final hypothesis linking oxygen and temperature places the emphasis on temperature fluctuations experienced by an organism rather than the maximum temperature of habitability. Physiological experiments on anthozoan cnidarians have revealed that hypoxia tolerance decreases not only at temperatures that are warmer than a species' specific environmental optimum (due to increased metabolic demand), but also at colder temperatures (Boag et al., 2018; see also Duncan et al., 2023; Endress et al., 2024; Pörtner, 2010). This increased oxygen requirement at cold temperatures is due to the lower diffusive potential of oxygen in cold seawater, as well as the amount of available energy that must be devoted to ventilation in colder, more viscous seawater. If atmospheric oxygen levels were relatively low in the early and middle Ediacaran, the shallow shelf—which is characterized by frequent diurnal and seasonal temperature swings—thus becomes an aerobically challenging environment, with every temperature change (hotter or colder) pushing animals into a state of hypoxia and preventing regular ecological function (Boag et al., 2018). Boag et al. (2018) consequently hypothesized that the Avalon assemblage inhabited the deeper ocean, despite the apparent downsides, for its environmental stability. Lack of appreciable temperature change (termed stenothermal) in the deep ocean would have then provided a refugium where organisms could optimize to live at oxygen levels only slightly above their minimal requirement (Boag et al., 2018). We note that these three hypotheses are not mutually exclusive but given the apparent permissibility of cold habitats in polar regions during the middle Ediacaran, we view the stenothermal hypothesis as the best explanation for the deep-water appearance of the Avalon assemblage.

In all the hypotheses outlined above, the Avalon assemblage was limited to the deep sea because of energetics—either low aerobic scope due to very hot temperatures or fluctuating temperatures, or low metabolic rates driven by limited chemical energy in the marine system. In this view, the radiation of Ediacaran animals onto the shelf in the ca. 560–550 Ma interval (White Sea) represents an increase in aerobic scope or available energy. A better understanding of how the environment may have changed, and thus affected the Ediacara biota, requires increased study of the White Sea time interval. As noted by Ostrander et al. (2023) and Rooney et al. (2020), an older age for the Shuram CIE means there is relatively little geochemical data from the actual time the White Sea biota flourished (at least based on published ages from siliciclastic successions in Russia (Martin et al., 2000)). Nonetheless, it is worthwhile discussing available geochemical data, specifically whether there was widespread oxygenation associated with the Shuram CIE that occurred between the Avalon and White Sea biotas. There is a clear positive uranium isotope excursion observed in carbonates during the CIE in many localities worldwide that has been interpreted as representing near-modern oxygenation (Zhang et al., 2019). However, more recent modeling by Gong et al. (2023) has suggested this could represent an expansion of anoxic but non-sulfidic ("ferruginous") conditions at this time rather than an expansion of oxic waters. This interpretation is primarily based on the observation that sediments deposited under ferruginous conditions often show a similar and negligible fractionation in uranium isotopes from seawater compared to oxic sediments (Cole, Planavsky, et al., 2020). Thallium isotopes, another redox-sensitive isotopic proxy, also do not show evidence for oxygenation either across the Shuram CIE or the Ediacaran more broadly (Ostrander et al., 2020, 2023; but see alternate interpretations of data from South China in Fan et al. (2020) and subsequent discussion in Ostrander et al. (2020)). Thus, although there may have been minor oxygenation in the middle Ediacaran (that could have still been biologically meaningful; Sperling, Knoll, & Girguis, 2015), current interpretations of geochemical data do not support widespread oxygenation. Consequently, we tentatively lean toward the effect of minor oxygenation coupled with synergistic changes in climate and/or primary productivity as being important in the upslope migration of Ediacaran organisms in the White Sea interval. The timing and climatic effects of possible late Ediacaran glaciation (e.g., Wang et al., 2023) are important in this regard, and further study of all three key drivers of animal energetics, and of the fossil record itself, are required to fully address such questions.

5 | CONCLUSIONS

The stratigraphic paleobiological study presented here from the Rackla Group of the Wernecke Mountains, NW Canada, represents the first basin-scale attempt to test whether the deep-ocean origination of the Ediacara biota represents a genuine evolutionary phenomenon in both geological time and space. These data demonstrate that the earliest complex macroscopic eukaryotes and animals in the fossil record were initially restricted to the deep ocean for ~15 Ma in an apparent refugium (Figure 10). As such, there is now geological support for the hypothesis that low oxygen and/or climatic conditions initially restricted early animals from inhabiting the shallow ocean during the Avalon interval > 574–560 Ma (Boag et al., 2018). Additionally, these data provide important new insight into the broader temporal and evolutionary history of the Ediacaran Period. Specifically, the middle Ediacaran origination of animals and large eukaryotes in the fossil record was not coincident with the beginning of the ca. 574–567 Ma Shuram CIE, but rather predates the excursion. Furthermore, the eventual migration of Ediacaran fauna up onto the shelf in White Sea time occurred after the termination of the Shuram CIE. These results have important implications for previous hypotheses which have suggested the Shuram CIE had a major role in facilitating the initial diversification of the Ediacara biota (e.g., Fike et al., 2006; Zhang et al., 2019). Future directions may now focus on providing new constraints on the chronology and geochemical conditions during the White Sea interval to understand whether environmental drivers were genuinely responsible for the magnitude and timing of metazoan diversification onto the shelves of the global oceans. These data can then be used to support or refute existing physiological models (e.g., Boag et al., 2018; Evans et al., 2018; Sperling & Stockey, 2018) linking the paleontological and geochemical records.

ACKNOWLEDGMENTS

This research took place in the traditional territory of the Na-Cho Nyäk Dun and we are grateful for their permission to work in the area. The research was supported by National Geographic Society (NGS) grant CP-102R-17 (awarded to EAS) and National Science Foundation (NSF) grants EAR-1654131 and EAR-2021176 (awarded to JVS), as well as the Geological Survey of Canada, the Yukon Geological Survey, and Yukon Paleontologist Grant Zazula. THB acknowledges support from a NSERC Doctoral Fellowship, the American Philosophical Society Lewis and Clark Fund, and Stanford McGee-Levorsen funds. JFB also acknowledges support from

NGS grant EC-393R-18, as well as graduate student grants from the American Philosophical Society Lewis and Clark fund and the Geological Society of America. THB, JTG, and EAS thank affiliates of the Stanford Project on Deepwater Depositional Systems. We thank Rob MacNaughton and Karen Fallas for sharing GSC helicopter resources, and their thoughtful discussions on our work. We thank David Moynihan for helpful discussions on Nadaleen River area stratigraphy, Guy Narbonne for discussion on the Ediacaran paleobiology of NW Canada, Andy Marquez, Murray Duncan, Richard Stockey, Curtis Deutsch, and Kyra Anderson for discussions of metazoan ecophysiology, Jack Taylor and Max Saylor for field assistance, and Guy Narbonne, Emmy Smith, and an anonymous reviewer for helpful comments on the manuscript. We also thank Fireweed Helicopters, Horizon Helicopters, and Great Slave Helicopters for safe flying in the mountains. Lastly, we thank the late Julia Lane, VP of Exploration for ATAC Resources, for her enthusiasm in Yukon geology and fieldwork and for coordinating support and helicopter time in support of this project. Any use of trade, firm, or product names is for descriptive purposes only and does not imply endorsement by the U.S. Government.

DATA AVAILABILITY STATEMENT

All data generated in this study are included in the main text.

ORCID

James F. Busch https://orcid.org/0000-0003-0816-8433
Jared T. Gooley https://orcid.org/0000-0001-5620-3702
Justin V. Strauss https://orcid.org/0000-0003-3298-3227
Erik A. Sperling https://orcid.org/0000-0001-9590-371X

REFERENCES

Aitken, J. D. (1989). Uppermost Proterozoic formations in Central Mackenzie Mountains, Northwest Territories. *Geological Survey of Canada Bulletin*, *368*, 1–24.

Arnott, R. W. C. (1992). Ripple cross-stratification in swaley cross-stratified sandstones of the Chungo Member, Mount Yamnuska, Alberta. *Canadian Journal of Earth Sciences*, *29*, 1802–1805.

Bergmann, K., Boekelheide, N., Clarke, J. W., Cantine, M. D., Wilcots, J., Anderson, N. T., Jost, A. B., Laub, O., Drozd, J., Goldberg, S. L., Mackey, T., Meyer, F., & Eyster, A. (2022). A billion years of temperature variability: A key driver of Earth's long-term habitability. *Earth and Space Science Open Archive*, essoar.10511918.3.

Bergmann, K., Osburn, M. R., Wilcots, J., Cantine, M., Grotzinger, J. P., Fischer, W. W., Eiler, J. M., & Bonifacie, M. (2022). The Shuram excursion: A response to climate extremes at the dawn of animal life. *Earth and Space Science Open Archive*, essoar.10511917.2.

Boag, T. H., Darroch, S. A. F., & Laflamme, M. (2016). Ediacaran distributions in space and time: Testing assemblage concepts of earliest macroscopic body fossils. *Paleobiology*, *42*, 574–594.

Boag, T. H., Stockey, R. G., Elder, L. E., Hull, P. M., & Sperling, E. A. (2018). Oxygen, temperature and the deep-marine stenothermal cradle of Ediacaran evolution. *Proceedings of the Royal Society B: Biological Sciences*, *285*, 20181724.

Bond, G. C., Christie-Blick, N., Kominz, M. A., & Devlin, W. J. (1985). An early Cambrian rift to post-rift transition in the Cordillera of western North America. *Nature*, *315*, 742–746.

Bowyer, F. T., Zhuravlev, A. Y., Wood, R., Shields, G. A., Zhou, Y., Curtis, A., Poulton, S. W., Condon, D. J., Yang, C., & Zhu, M. (2022). Calibrating the temporal and spatial dynamics of the Ediacaran – Cambrian radiation of animals. *Earth-Science Reviews*, *225*(103), 913.

Burzynski, G., & Narbonne, G. M. (2015). The discs of Avalon: Relating discoid fossils to frondose organisms in the Ediacaran of Newfoundland, Canada. *Palaeogeography, Palaeoclimatology, Palaeoecology, Ediacaran Environments and Ecosystems*, *434*, 34–45.

Busch, J. F., Boag, T. H., Sperling, E. A., Rooney, A. D., Feng, X., Moynihan, D. P., & Strauss, J. V. (2023). Integrated litho-, chemo- and sequence stratigraphy of the Ediacaran Gametrail Formation across a shelf-slope transect in the Wernecke Mountains, Yukon, *Canada. American Journal of Science*, *323*, 4.

Busch, J. F., Hodgin, E. B., Ahm, A.-S. C., Husson, J. M., Macdonald, F. A., Bergmann, K. D., Higgins, J. A., & Strauss, J. V. (2022). Global and local drivers of the Ediacaran Shuram carbon isotope excursion. *Earth and Planetary Science Letters*, *579*, 117368.

Busch, J. F., Rooney, A. D., Meyer, E. E., Town, C. F., Moynihan, D. P., & Strauss, J. V. (2021). Late Neoproterozoic – early Paleozoic basin evolution in the Coal Creek inlier of Yukon, Canada: Implications for the tectonic evolution of northwestern Laurentia. *Canadian Journal of Earth Sciences*, *58*, 355–377.

Canfield, D. E., Knoll, A. H., Poulton, S. W., Narbonne, G. M., & Dunning, G. R. (2020). Carbon isotopes in clastic rocks and the Neoproterozoic carbon cycle. *American Journal of Science*, *320*, 97–124.

Carbone, C., & Narbonne, G. M. (2014). When life got smart: The evolution of behavioral complexity through the Ediacaran and early Cambrian of NW Canada. *Journal of Paleontology*, *88*, 309–330.

Carbone, C. A., Narbonne, G. M., Macdonald, F. A., & Boag, T. H. (2015). New Ediacaran fossils from the uppermost Blueflower Formation, northwest Canada: Disentangling biostratigraphy and paleoecology. *Journal of Paleontology*, *89*, 281–291.

Cecile, M. P. (2000). Geology of the northeastern Niddery Lake map area, east-central yukon and adjacent northwest territories. *Bulletin of the Geological Survey of Canada*, *553*, 1–119.

Cole, D. B., Mills, D. B., Erwin, D. H., Sperling, E. A., Porter, S. M., Reinhard, C. T., & Planavsky, N. J. (2020). On the co-evolution of surface oxygen levels and animals. *Geobiology*, *18*, 260–281.

Cole, D. B., Planavsky, N. J., Longley, M., Böning, P., Wilkes, D., Wang, X., Swanner, E. D., Wittkop, C., Loydell, D., & Busigny, V. (2020). Uranium isotope fractionation in non-sulfidic anoxic settings and the global uranium isotope mass balance. *Global Biogeochemical Cycles*, *34*, e2020GB006649.

Dalrymple, R. W. (1979). Wave-induced liquefaction: A modern example from the Bay of Fundy. *Sedimentology*, *26*, 835–844.

Dalrymple, R. W., & Narbonne, G. M. (1996). Continental slope sedimentation in the Sheepbed formation (Neoproterozoic, Windermere Supergroup), Mackenzie Mountains, N.W.T. *Canadian Journal of Earth Sciences*, *33*, 848–862.

Darroch, S. A. F., Boag, T. H., Racicot, R. A., Tweedt, S., Mason, S. J., Erwin, D. H., & Laflamme, M. (2016). A mixed Ediacaran-metazoan assemblage from the Zaris Sub-basin, Namibia. *Palaeogeography, Palaeoclimatology, Palaeoecology*, *459*, 198–208.

Darroch, S. A. F., Cribb, A. T., Buatois, L. A., Germs, G. J. B., Kenchington, C. G., Smith, E. F., Mocke, H., O'Neil, G. R., Schiffbauer, J. D., Maloney, K. M., Racicot, R. A., Turk, K. A., Gibson, B. M., Almond, J., Koester, B., Boag, T. H., Tweedt, S. M., & Laflamme, M. (2021). The trace fossil record of the Nama Group, Namibia: Exploring the terminal Ediacaran roots of the Cambrian explosion. *Earth-Science Reviews*, *212*, 103435.

Darroch, S. A. F., Laflamme, M., Schiffbauer, J. D., & Briggs, D. E. G. (2012). Experimental formation of a microbial death mask. *PALAIOS*, *27*, 293–303.

Darroch, S. A. F., Smith, E. F., Laflamme, M., & Erwin, D. H. (2018). Ediacaran extinction and Cambrian explosion. *Trends in Ecology & Evolution*, *33*, 653–663.

Darroch, S. A. F., Sperling, E. A., Boag, T. H., Racicot, R. A., Mason, S. J., Morgan, A. S., Tweedt, S., Myrow, P., Johnston, D. T., Erwin, D. H., &

Laflamme, M. (2015). Biotic replacement and mass extinction of the Ediacara biota. *Proceedings of the Royal Society B*, *282*, 814.

Derry, L. A. (2015). Causes and consequences of mid-Proterozoic anoxia. *Geophysical Research Letters*, *42*, 8538–8546.

Deutsch, C., Ferrel, A., Seibel, B., Pörtner, H.-O., & Huey, R. B. (2015). Climate change tightens a metabolic constraint on marine habitats. *Science*, *348*, 1132–1135.

Droser, M. L., Evans, S. D., Tarhan, L. G., Surprenant, R. L., Hughes, I. V., Hughes, E. B., & Gehling, J. G. (2022). What happens between depositional events, stays between depositional events: The significance of organic mat surfaces in the capture of Ediacara communities and the sedimentary rocks that preserve them. *Frontiers in Earth Science*, *10*, 826353.

Duke, W. L. (1985). Hummocky cross-stratification, tropical hurricanes, and intense winter storms. *Sedimentology*, *32*, 167–194.

Duncan, M. I., Micheli, F., Boag, T. H., Marquez, J. A., Deres, H., Deutsch, C. A., & Sperling, E. A. (2023). Oxygen availability and body mass modulate ectotherm responses to ocean warming. *Nature Communications*, *14*, 3811.

Endress, M.-G. A., Boag, T. H., Burford, B. P., Penn, J. L., Sperling, E. A., & Deutsch, C. A. (2024). Physiological causes and biogeographic consequences of thermal optima in the hypoxia tolerance of marine ectotherms. *PLoS Biology*, *22*, e3002443.

Evans, S. D., Diamond, C. W., Droser, M. L., & Lyons, T. W. (2018). Dynamic oxygen and coupled biological and ecological innovation during the second wave of the Ediacara biota. *Emerging Topics in Life Sciences*, *2*, 223–233.

Evans, S. D., Hughes, I. V., Gehling, J. G., & Droser, M. L. (2020). Discovery of the oldest bilaterian from the Ediacaran of South Australia. *Proceedings of the National Academy of Sciences*, *117*, 7845–7850.

Evans, S. D., Tu, C., Rizzo, A., Surprenant, R. L., Boan, P. C., McCandless, H., Marshall, N., Xiao, S., & Droser, M. L. (2022). Environmental drivers of the first major animal extinction across the Ediacaran White Sea-Nama transition. *Proceedings of the National Academy of Sciences*, *119*, e2207475119.

Fan, H., Nielsen, S. G., Owens, J. D., Auro, M., Shu, Y., Hardisty, D. S., Horner, T. J., Bowman, C. N., Young, S. A., & Wen, H. (2020). Constraining oceanic oxygenation during the Shuram excursion in South China using thallium isotopes. *Geobiology*, *18*, 348–365.

Fedonkin, M. A. (2003). The origin of the Metazoa in the light of the Proterozoic fossil record. *Paleontological Research*, *7*, 9–41.

Fike, D. A., Grotzinger, J. P., Pratt, L. M., & Summons, R. E. (2006). Oxidation of the Ediacaran ocean. *Nature*, *444*, 744–747.

Fitzgerald, D. M., Narbonne, G. M., Pufahl, P. K., & Dalrymple, R. W. (2024). The Mall Bay Formation (Ediacaran) and the protracted onset of the Gaskiers glaciation in Newfoundland, Canada. *Precambrian Research*, *405*, 107369.

Fritz, W. H., Narbonne, G. M., & Gordey, S. P. (1983). Strata and trace fossils near the Precambrian-Cambrian boundary, Mackenzie, Selwyn, and Wernecke Mountains, Yukon and Northwest Territories. *Current Research, Part B, Geological Survey of Canada, Paper*, *84–1B*, 365–375.

Gardiner, S. (1984). *Sedimentology and local basin analysis of the lower Conception Group (Hadrynian), Avalon Zone, Newfoundland* (masters).

Gehling, J. G. (1999). Microbial mats in terminal Proterozoic siliciclastics: Ediacaran death masks. *PALAIOS*, *14*, 40–57.

Gehling, J. G., & Droser, M. L. (2009). Textured organic surfaces associated with the Ediacara biota in South Australia. *Earth-Science Reviews*, *96*, 196–206.

Gehling, J. G., & Droser, M. L. (2013). How well do fossil assemblages of the Ediacara biota tell time? *Geology*, *41*, 447–450.

Gehling, J. G., Narbonne, G. M., & Anderson, M. M. (2000). The first named Ediacaran body fossil, *Aspidella terranovica*. *Palaeontology*, *43*, 427–456.

Gillooly, J. F., Brown, J. H., West, G. B., Savage, V. M., & Charnov, E. L. (2001). Effects of size and temperature on metabolic rate. *Science*, *293*, 2248–2251.

Goldberg, S. L., Present, T. M., Finnegan, S., & Bergmann, K. D. (2021). A high-resolution record of early Paleozoic climate. *Proceedings of the National Academy of Sciences*, *118*, e2013083118.

Gong, Z., Wei, G.-Y., Fakhraee, M., Alcott, L. J., Jiang, L., Zhao, M., & Planavsky, N. J. (2023). Revisiting marine redox conditions during the Ediacaran Shuram carbon isotope excursion. *Geobiology*, *21*, 407–420.

Grazhdankin, D. (2004). Patterns of distribution in the Ediacaran biotas: Facies versus biogeography and evolution. *Paleobiology*, *30*, 203–221.

Grazhdankin, D. (2014). Patterns of evolution of the Ediacaran soft-bodied biota. *Journal of Paleontology*, *88*, 269–283.

Hearing, T. W., Harvey, T. H. P., Williams, M., Leng, M. J., Lamb, A. L., Wilby, P. R., Gabbott, S. E., Pohl, A., & Donnadieu, Y. (2018). An early Cambrian greenhouse climate. *Science Advances*, *4*, eaar5690.

Hoffman, P. F., & Li, Z. X. (2009). A paleogeographic context for Neoproterozoic glaciation. *Palaeogeography, Palaeoclimatology, Palaeoecology*, *277*, 158–172.

Hofmann, H. J. (1981). First record of a Late Proterozoic faunal assemblage in the North American Cordillera. *Lethaia*, *14*, 303–310.

Hofmann, H. J., Fritz, W. H., & Narbonne, G. M. (1983). Ediacaran (Precambrian) fossils from the Wernecke Mountains, northwestern Canada. *Science*, *221*, 455–457.

Holland, S. M. (1995). The stratigraphic distribution of fossils. *Paleobiology*, *21*, 92–109.

Hua, H., Zhang, L. Y., Zhang, Z. F., & Wang, J. P. (2000). Fossil evidence of latest Neoproterozoic Gaojiashan biota and their characteristics. *Acta Palaeontologica Sinica*, *39*, 507–515.

Ichaso, A. A., Dalrymple, R. W., & Narbonne, G. M. (2007). Paleoenvironmental and basin analysis of the late Neoproterozoic (Ediacaran) upper Conception and St. John's groups, west Conception Bay, Newfoundland. *Canadian Journal of Earth Sciences*, *44*, 25–41.

Jablonski, D., Sepkoski, J. J., Bottjer, D. J., & Sheehan, P. M. (1983). Onshore-offshore patterns in the evolution of Phanerozoic shelf communities. *Science (New York, N.Y.)*, *222*, 1123–1125.

James, N. P., Narbonne, G. M., & Kyser, T. K. (2001). Late Neoproterozoic cap carbonates: Mackenzie Mountains, northwestern Canada: Precipitation and global glacial meltdown. *Canadian Journal of Earth Sciences*, *38*, 1229–1262.

Jelby, M. E., Grundvåg, S.-A., Helland-Hansen, W., Olaussen, S., & Stemmerik, L. (2020). Tempestite facies variability and storm-depositional processes across a wide ramp: Towards a polygenetic model for hummocky cross-stratification. *Sedimentology*, *67*, 742–781.

Krause, A. J., Mills, B. J. W., Merdith, A. S., Lenton, T. M., & Poulton, S. W. (2022). Extreme variability in atmospheric oxygen levels in the late Precambrian. *Science Advances*, *8*, eabm8191.

Laakso, T. A., & Schrag, D. P. (2018). A small marine biosphere in the Proterozoic. *Geobiology*, *17*, 161–171.

Laflamme, M., & Narbonne, G. M. (2008). Ediacaran fronds. *Palaeogeography, Palaeoclimatology, Palaeoecology*, *258*, 162–179.

Laflamme, M., Schiffbauer, J. D., & Narbonne, G. M. (2012). Deep-water Microbially induced sedimentary structures (MISS) in deep time: The Ediacaran fossil Ivesheadia. In N. Noffke & H. Chafetz (Eds.), *Microbial Mats in siliciclastic depositional systems through time*. SEPM Society for Sedimentary Geology.

Lear, K. O., Morgan, D. L., Whitty, J. M., Whitney, N. M., Byrnes, E. E., Beatty, S. J., & Gleiss, A. C. (2020). Divergent field metabolic rates highlight the challenges of increasing temperatures and energy limitation in aquatic ectotherms. *Oecologia*, *193*, 311–323.

Li, C., Hardisty, D. S., Luo, G., Huang, J., Algeo, T. J., Cheng, M., Shi, W., An, Z., Tong, J., Xie, S., Jiao, N., & Lyons, T. W. (2017). Uncovering the spatial heterogeneity of Ediacaran carbon cycling. *Geobiology*, *15*, 211–224.

Liu, A. G., Kenchington, C. G., & Mitchell, E. G. (2015). Remarkable insights into the paleoecology of the Avalonian Ediacaran macrobiota. *Gondwana Research*, *27*, 1355–1380.

Liu, A. G., Matthews, J. J., Menon, L. R., McIlroy, D., & Brasier, M. D. (2014). Haootia quadriformis n. gen., n. sp., interpreted as a muscular cnidarian impression from the Late Ediacaran period (approx. 560 Ma). *Proceedings of the Royal Society B: Biological Sciences*, *281*, 20141202.

Liu, A. G., McIlroy, D., Mathews, J. J., & Brasier, M. D. (2012). A new assemblage of juvenile Ediacaran fronds from the Drook Formation, Newfoundland. *Journal of the Geological Society*, *169*, 395–403.

Lu, W., Ridgwell, A., Thomas, E., Hardisty, D. S., Luo, G., Algeo, T. J., Saltzman, M. R., Gill, B. C., Shen, Y., Ling, H.-F., Edwards, C. T., Whalen, M. T., Zhou, X., Gutchess, K. M., Jin, L., Rickaby, R. E. M., Jenkyns, H. C., Lyons, T. W., Lenton, T. M., … Lu, Z. (2018). Late inception of a resiliently oxygenated upper ocean. *Science*, *361*, 174–177.

Macdonald, F. A., Schmitz, M. D., Strauss, J. V., Halverson, G. P., Gibson, T. M., Eyster, A., Cox, G., Mamrol, P., & Crowley, J. L. (2018). Cryogenian of Yukon. *Precambrian Research*, *319*, 114–143.

Macdonald, F. A., Strauss, J. V., Sperling, E. A., Halverson, G. P., Narbonne, G. M., Johnston, D. T., Kunzmann, M., Schrag, D. P., & Higgins, J. A. (2013). The stratigraphic relationship between the Shuram carbon isotope excursion, the oxygenation of Neoproterozoic oceans, and the first appearance of the Ediacara biota and bilaterian trace fossils in northwestern Canada. *Chemical Geology*, *362*, 250–272.

MacNaughton, R. (2020). Neoproterozoic–Cambrian stratigraphy of the Mackenzie Mountains, northwestern Canada, part I: Ediacaran measured sections and updated lithostratigraphy, NE Sekwi Mountain map area (NTS 105-P), *Geological Survey of Canada Open File*, *7315*, 1-22.

MacNaughton, R., & Fallas, K. (2021). Neoproterozoic–Cambrian stratigraphy of the Mackenzie Mountains, northwestern Canada, part IV: A stratigraphic reference section for the Ediacaran–Cambrian transition in NTS 95-M (Wrigley Lake map area), *Geological Survey of Canada Open File*, *8839*, 1–58.

MacNaughton, R. B., Fallas, K. M., Martell, J., & Edgeworth, I. (2018). Bedrock mapping, stratigraphy, and related studies, Bonnet Plume Lake (NTS 106-B) and Wrigley Lake (NTS 95-M) map areas, Northwest Territories and Yukon: GEM-2 Mackenzie Project, report of activities 2018. *Geological Survey of Canada Open File*, *8471*, 1–17.

MacNaughton, R., Roots, C. F., & Martel, E. (2008). *Neoproterozoic-(?) Cambrian lithostratigraphy, northeast Sekwi Mountain map area, Mackenzie Mountains, Northwest Territories: New data from measured sections*. Natural Resources Canada.

MacNaughton, R. B., Narbonne, G. M., & Dalrymple, R. W. (2000). Neoproterozoic slope deposits, Mackenzie Mountains, northwestern Canada: Implications for passive-margin development and Ediacaran faunal ecology. *Canadian Journal of Earth Sciences*, *37*, 997–1020.

Marsay, C. M., Sanders, R. J., Henson, S. A., Pabortsava, K., Achterberg, E. P., & Lampitt, R. S. (2015). Attenuation of sinking particulate organic carbon flux through the mesopelagic ocean. *Proceedings of the National Academy of Sciences of the United States of America*, *112*, 1089–1094.

Martin, M. W., Grazhdankin, D. V., Bowring, S. A., Evans, D. A. D., Fedonkin, M. A., & Kirschvink, J. L. (2000). Age of Neoproterozoic bilaterian body and trace fossils, White Sea, Russia: Implications for metazoan evolution. *Science*, *288*, 841–845.

Matthews, J. J., Liu, A. G., Yang, C., McIlroy, D., Levell, B., & Condon, D. J. (2020). A chronostratigraphic framework for the rise of the Ediacaran macrobiota: New constraints from Mistaken Point Ecological Reserve, Newfoundland. *Geological Society of America Bulletin*, *133*, 612–624.

McMahon, W. J., Liu, A. G., Tindal, B. H., & Keinhans, M. G. (2020). Ediacaran life close to land: Coastal and shoreface habitats of the Ediacaran macrobiota, the Central Flinders ranges, South Australia. *Journal of Sedimentary Research*, *90*, 1463–1499.

Merdith, A. S., Williams, S. E., Collins, A. S., Tetley, M. G., Mulder, J. A., Blades, M. L., Young, A., Armistead, S. E., Cannon, J., Zahirovic, S., & Müller, R. D. (2021). Extending full-plate tectonic models into deep time: Linking the Neoproterozoic and the Phanerozoic. *Earth-Science Reviews*, *214*(103), 477.

Moynihan, D. P., Strauss, J. V., Nelson, L. L., & Padget, C. D. (2019). Upper Windermere Supergroup and the transition from rifting to continent-margin sedimentation, Nadaleen River area, northern Canadian Cordillera. *Geological Society of America Bulletin*, *131*, 1673–1701.

Muscente, A. D., Boag, T. H., Bykova, N., & Schiffbauer, J. D. (2018). Environmental disturbance, resource availability, and biologic turnover at the dawn of animal life. *Earth-Science Reviews*, *177*, 248–264.

Myrow, P. M. (1992). Pot and gutter casts from the Chapel Island Formation, Southeast Newfoundland. *Journal of Sedimentary Research*, *62*, 992–1007.

Narbonne, G. M. (1994). New Ediacaran fossils from the Mackenzie Mountains, northwestern Canada. *Journal of Paleontology*, *68*, 411–416.

Narbonne, G. M. (2005). The Ediacara biota: Neoproterozoic origin of animals and their ecosystems. *Annual Review in Earth and Planetary Sciences*, *33*, 421–442.

Narbonne, G. M., & Aitken, J. D. (1990). Ediacaran fossils from the Sekwi brook area, Mackenzie Mountains, northwestern Canada. *Palaeontology*, *33*, 945–980.

Narbonne, G. M., & Gehling, J. G. (2003). Life after Snowball: The oldest complex Ediacaran fossils. *Geology*, *31*, 27–30.

Narbonne, G. M., & Hofmann, H. J. (1987). Ediacaran biota of the Wernecke Mountains, Yukon, Canada. *Palaeontology*, *30*, 647–676.

Narbonne, G. M., Laflamme, M., Trusler, P. W., Dalrymple, R. W., & Greentree, C. (2014). Deep-water Ediacaran fossils from northwestern Canada: Taphonomy, ecology, and evolution. *Journal of Paleontology*, *88*, 207–223.

Nelson, L. L., Crowley, J. L., Smith, E. F., Schwartz, D. M., Hodgin, E. B., & Schmitz, M. D. (2023). Cambrian explosion condensed: High-precision geochronology of the lower Wood Canyon Formation, Nevada. *Proceedings of the National Academy of Sciences*, *120*, e2301478120.

Nelson, L. L., Ramezani, J., Almond, J. E., Darroch, S. A. F., Taylor, W. L., Brenner, D. C., Furey, R. P., Turner, M., & Smith, E. F. (2022). Pushing the boundary: A calibrated Ediacaran-Cambrian stratigraphic record from the Nama Group in northwestern Republic of South Africa. *Earth and Planetary Science Letters*, *580*(117), 396.

Noble, S. R., Condon, D. J., Carney, J. N., Wilby, P. R., Pharaoh, T. C., & Ford, T. D. (2015). U–Pb geochronology and global context of the Charnian Supergroup, UK: constraints on the age of key Ediacaran fossil assemblages. *Geological Society of America Bulletin*, *127*, 250–265.

Nowlan, G. S., Narbonne, G. M., & Fritz, W. H. (1985). Small shelly fossils and trace fossils near the Precambrian-Cambrian boundary in the Yukon Territory, Canada. *Lethaia*, *18*, 233–256.

Ostrander, C. M. (2023). Mulling and nulling the coeval rise of Ediacaran oxygen and animals. *Earth and Planetary Science Letters*, *614*, 118187.

Ostrander, C. M., Bjerrum, C. J., Ahm, A.-S. C., Stenger, S. R., Bergmann, K. D., El-Ghali, M. A. K., Harthi, A. R., Aisri, Z., & Nielsen, S. G. (2023). Widespread seafloor anoxia during generation of the Ediacaran Shuram carbon isotope excursion. *Geobiology*, *21*, 556–570.

Ostrander, C. M., Owens, J. D., Nielsen, S. G., Lyons, T. W., Shu, Y., Chen, X., Sperling, E. A., Jiang, G., Johnston, D. T., Sahoo, S. K., & Anbar, A. D. (2020). Thallium isotope ratios in shales from South China and northwestern Canada suggest widespread O_2 accumulation in marine bottom waters was an uncommon occurrence during the Ediacaran period. *Chemical Geology*, *557*(119), 856.

Ozaki, K., Reinhard, C. T., & Tajika, E. (2019). A sluggish mid-Proterozoic biosphere and its effect on Earth's redox balance. *Geobiology*, *17*, 3–11.

Patzkowsky, M. E., & Holland, S. M. (2012). *Stratigraphic Paleobiology: Understanding the distribution of fossil taxa in time and space*. University of Chicago Press.

Pörtner, H.-O. (2010). Oxygen- and capacity-limitation of thermal tolerance: A matrix for integrating climate-related stressor effects in marine ecosystems. *Journal of Experimental Biology*, *213*, 881–893.

Pu, J. P., Bowring, S. A., Ramezani, J., Myrow, P., Raub, T. D., Landing, E., Mills, A., Hodgin, E., & Macdonald, F. A. (2016). Dodging snowballs: Geochronology of the Gaskiers glaciation and the first appearance of the Ediacaran biota. *Geology*, *44*, 955–958.

Pyle, L. J., Narbonne, G. M., James, N. P., Dalrymple, R. W., & Kaufman, A. J. (2004). Integrated Ediacaran chronostratigraphy, Wernecke Mountains, northwestern Canada. *Precambrian Research*, *132*, 1–27.

Pyle, L. J., Narbonne, G. M., Nowlan, G. S., Xiao, S., & James, N. P. (2006). Early Cambrian metazoan eggs, embryos, and phosphatic microfossils from northwestern Canada. *Journal of Paleontology*, *80*, 811–825.

Reinhard, C. T., Planavsky, N. J., Gill, B. C., Ozaki, K., Robbins, L. J., Lyons, T. W., Fischer, W. W., Wang, C., Cole, D. B., & Konhauser, K. O. (2017). Evolution of the global phosphorus cycle. *Nature*, *541*, 386–389.

Rooney, A. D., Cantine, M. D., Bergmann, K. D., Gómez-Pérez, I., Al Baloushi, B., Boag, T. H., Busch, J. F., Sperling, E. A., & Strauss, J. V. (2020). Calibrating the coevolution of Ediacaran life and environment. *Proceedings of the National Academy of Sciences*, *117*, 16824–16830.

Rooney, A. D., Strauss, J. V., Brandon, A. D., & Macdonald, F. A. (2015). A Cryogenian chronology: Two long-lasting synchronous Neoproterozoic glaciations. *Geology*, *43*, 459–462.

Schiffbauer, J., Huntley, J., O'Neil, G. R., Darroch, S., Laflamme, M., & Cai, Y. (2016). The latest Ediacaran Wormworld Fauna: Setting the ecological stage for the Cambrian explosion. *GSA Today*, *26*, 4–11.

Schulte, P. M. (2015). The effects of temperature on aerobic metabolism: Towards a mechanistic understanding of the responses of ectotherms to a changing environment. *The Journal of Experimental Biology*, *218*, 1856–1866.

Seilacher, A. (1999). Biomat-related lifestyles in the Precambrian. *PALAIOS*, *14*, 86–93.

Simpson, C. (2021). Adaptation to a viscous Snowball Earth ocean as a path to complex multicellularity. *The American Naturalist*, *198*, 590–609.

Slagter, S., Hao, W., Planavsky, N. J., Konhauser, K. O., & Tarhan, L. G. (2022). Biofilms as agents of Ediacara-style fossilization. *Scientific Reports*, *12*, 8631.

Smith, C. R., De Leo, F. C., Bernardino, A. F., Sweetman, A. K., & Arbizu, P. M. (2008). Abyssal food limitation, ecosystem structure and climate change. *Trends in Ecology & Evolution*, *23*, 518–528.

Smith, E. F., Nelson, L. L., Strange, M. A., Eyster, A. E., Rowland, S. M., Schrag, D. P., & Macdonald, F. A. (2016). The end of the Ediacaran: Two new exceptionally preserved body fossil assemblages from Mount Dunfee, Nevada, USA. *Geology*, *44*, 911–914.

Sperling, E. A., Boag, T. H., Duncan, M. I., Endriga, C. R., Marquez, J. A., Mills, D. B., Monarrez, P. M., Sclafani, J. A., Stockey, R. G., & Payne, J. L. (2022). Breathless through time: Oxygen and animals through Earth's history. *Biological Bulletin*, *243*, 184–206.

Sperling, E. A., Carbone, C., Strauss, J. V., Johnston, D. T., Narbonne, G. M., & Macdonald, F. A. (2016). Oxygen, facies, and secular controls on the appearance of Cryogenian and Ediacaran body and trace fossils in the Mackenzie Mountains of northwestern Canada. *Geological Society of America Bulletin*, *128*, 558–575.

Sperling, E. A., Knoll, A. H., & Girguis, P. R. (2015). The ecological physiology of Earth's second oxygen revolution. *Annual Review of Ecology, Evolution, and Systematics*, *46*, 215–235.

Sperling, E. A., Peterson, K. J., & Laflamme, M. (2011). Rangeomorphs, Thectardis (Porifera?) and dissolved organic carbon in the Ediacaran oceans. *Geobiology*, *9*, 24–33.

Sperling, E. A., & Stockey, R. G. (2018). The temporal and environmental context of early animal evolution: considering all the ingredients of an "explosion.". *Integrative and Comparative Biology*, *58*, 605–622.

Sperling, E. A., & Vinther, J. (2010). A placozoan affinity for Dickinsonia and the evolution of late Proterozoic metazoan feeding modes. *Evolution and Development*, *12*, 201–207.

Sperling, E. A., Wolock, C. J., Morgan, A. S., Gill, B. C., Kunzmann, M., Halverson, G. P., Macdonald, F. A., Knoll, A. H., & Johnston, D. T. (2015). Statistical analysis of iron geochemical data suggests limited late Proterozoic oxygenation. *Nature*, *523*, 451–454.

Ste-Marie, E., Watanabe, Y. Y., Semmens, J. M., Marcoux, M., & Hussey, N. E. (2022). Life in the slow lane: Field metabolic rate and prey consumption rate of the Greenland shark (Somniosus microcephalus) modelled using archival biologgers. *Journal of Experimental Biology*, *225*, jeb242994.

Stockey, R. G., Pohl, A., Ridgwell, A., Finnegan, S., & Sperling, E. A. (2021). Decreasing Phanerozoic extinction intensity as a consequence of Earth surface oxygenation and metazoan ecophysiology. *Proceedings of the National Academy of Sciences*, *118*, e2101900118.

Stolper, D. A., & Keller, C. B. (2018). A record of deep-ocean dissolved O_2 from the oxidation state of iron in submarine basalts. *Nature*, *553*, 323–327.

Strauss, J. V., MacDonald, F. A., Halverson, G. P., Tosca, N. J., Schrag, D. P., & Knoll, A. H. (2015). Stratigraphic evolution of the Neoproterozoic Callison Lake Formation: Linking the break-up of Rodinia to the Islay carbon isotope excursion. *American Journal of Science*, *315*, 881–944.

Tarhan, L. G., Droser, M. L., & Gehling, J. G. (2022). Picking out the warp and weft of the Ediacaran seafloor: Paleoenvironment and paleoecology of an Ediacara textured organic surface. *Precambrian Research*, *369*(106), 539.

Tarhan, L. G., Droser, M. L., Gehling, J. G., & Dzaugis, M. P. (2017). Microbial mat sandwiches and other anactualistic sedimentary features of the Ediacara Member (Rawnsley Quartzite, South Australia): Implications for interpretation of the Ediacaran sedimentary record. *PALAIOS*, *32*, 181–194.

Verberk, W. C. E. P., Bilton, D. T., Piero, C., & Spicer, J. I. (2011). Oxygen supply in aquatic ectotherms: Partial pressure and solubility together explain biodiversity and size patterns. *Ecology*, *92*, 1565–1572.

Waggoner, B. (2003). The Ediacaran biota in space and time. *Integrative and Comparative Biology*, *43*, 104–113.

Wang, R., Yin, Z., & Shen, B. (2023). A late Ediacaran ice age: The key node in the Earth system evolution. *Earth-Science Reviews*, *247*, 104610.

Wilby, P. R., Carney, J. N., & Howe, M. P. A. (2011). A rich Ediacaran assemblage from eastern Avalonia: Evidence of early widespread diversity in the deep ocean. *Geology*, *39*, 655–658.

Wood, D. A., Dalrymple, R. W., Narbonne, G. M., Gehling, J. G., & Clapham, M. E. (2003). Paleoenvironmental analysis of the late Neoproterozoic Mistaken Point and Trepassey formations, southeastern Newfoundland. *Canadian Journal of Earth Sciences*, *40*, 1375–1391.

Woods, H. A., Moran, A. L., Atkinson, D., Audzijonyte, A., Berenbrink, M., Borges, F. O., Burnett, K. G., Burnett, L. E., Coates, C. J., Collin, R., Costa-Paiva, E. M., Duncan, M. I., Ern, R., Laetz, E. M. J., Levin, L. A., Lindmark, M., Lucey, N. M., McCormick, L. R., Pierson, J. J., … Verberk, W. C. E. P. (2022). Integrative approaches to understanding organismal responses to aquatic deoxygenation. *The Biological Bulletin*, *243*, 85–103.

Woolley, S. N. C., Tittensor, D. P., Dunstan, P. K., Guillera-Arroita, G., Lahoz-Monfort, J. J., Wintle, B. A., Worm, B., & O'Hara, T. D. (2016). Deep-sea diversity patterns are shaped by energy availability. *Nature*, *533*, 393–396.

Xiao, S., & Laflamme, M. (2009). On the eve of animal radiation: Phylogeny, ecology and evolution of the Ediacaran biota. *Trends in Ecology & Evolution*, *24*, 31–40.

Xiao, S., Narbonne, G. M., Zhou, C., Laflamme, M., Grazhdankin, D. V., Moczydlowska-Vidal, M., & Cui, H. (2016). Towards an Ediacaran time scale: Problems, protocols, and prospects. *Episodes Journal of International Geoscience*, *39*, 540–555.

Xing, Y., Ding, Q., Luo, H., He, T., & Wang, Y. (1984). The Sinian-Cambrian boundary of China. *Bulletin of the Institute of Geology Chinese Academy of Geological Sciences*, *10*, 1–262.

Zhang, F., Xiao, S., Romaniello, S. J., Hardisty, D., Li, C., Melezhik, V., Pokrovsky, B., Cheng, M., Shi, W., Lenton, T. M., & Anbar, A. D. (2019). Global marine redox changes drove the rise and fall of the Ediacara biota. *Geobiology*, *17*, 594–610.

How to cite this article: Boag, T. H., Busch, J. F., Gooley, J. T., Strauss, J. V., & Sperling, E. A. (2024). Deep-water first occurrences of Ediacara biota prior to the Shuram carbon isotope excursion in the Wernecke Mountains, Yukon, Canada. *Geobiology*, *22*, e12597. https://doi.org/10.1111/gbi.12597